Boron-dependent posttranscriptional regulation of a borate transporter *BOR1* and its physiological significance in *Arabidopsis thaliana*

シロイヌナズナにおけるホウ酸輸送体 *BOR1* の
ホウ素濃度依存的な転写後制御とその生理的意義

Izumi Aibara
相原　いづみ

Division of Biosphere Science,
Graduate School of Environmental Science,
Hokkaido University

2018

CONTENTS

Introduction section is partly based on the paper published at:
Aibara I, Miwa K (2014) Strategies for optimization of mineral nutrient transport in plants: multilevel regulation of nutrient-dependent dynamics of root architecture and transporter activity. Plant Cell Physiol 55: 2027-2036

CHAPTER 1, CHAPTER 2 and a part of introduction are based on the study published at:
Aibara I, Hirai T, Kasai K, Takano J, Onouchi H, Naito S, Fujiwara T, Miwa, K (2018) Boron-dependent translational suppression of the borate exporter *BOR1* contributes to the avoidance of boron toxicity. Plant Physiology 177: 759-774 (Copyright American Society of Plant Biologists)

学 位 論 文 内 容 の 要 旨

博士（環境科学）　　氏　名　相原　いづみ

学 位 論 文 題 名

Boron-dependent posttranscriptional regulation of a borate transporter *BOR1* and its physiological significance in *Arabidopsis thaliana*

（シロイヌナズナにおけるホウ酸輸送体*BOR1*のホウ素濃度依存的な転写後制御とその生理的意義）

【背景】

植物は土壌中の変動する無機栄養環境に適応することが必要である。ホウ素は植物の微量必須元素であり、また、過剰に存在すると毒性を示す。そのため、植物は体内のホウ素濃度を過不足のない範囲に厳密に調節する必要がある。シロイヌナズナのホウ酸排出型輸送体であるBOR1は、低濃度ホウ素条件において根から地上部へのホウ素の移行に貢献する。*BOR1* のmRNA量は環境中のホウ素濃度によって変化しないが、BOR1タンパク質は低濃度ホウ素条件で根において蓄積し、ホウ素が十分存在する環境では蓄積量が減少する。このホウ素濃度依存的な発現の分子機構として、通常ホウ素条件におけるBOR1の選択的なタンパク質分解が示されていた。しかし一方で、それ以外の制御の存在も示唆されていた。本学位論文では（１）選択的タンパク質分解とは異なる*BOR1* のホウ素濃度依存的な発現制御の機構を明らかにし、（２）これらの発現制御のホウ素環境への適応における意義を示すことを目的とした。

【1. *BOR1* のホウ素濃度依存的な発現制御の分子機構】

選択的タンパク質分解とは異なる発現制御機構を明らかにするため、翻訳に注目した。真

核生物では一般的に、mRNAの上流配列である5′ 非翻訳領域（5′-UTR）が翻訳効率に関わることが知られている。*In vivo* と *in vitro* のレポーターアッセイから、*BOR1* の5′-UTR (356 nt) がホウ素濃度依存的な翻訳抑制に必要かつ十分であることが示された。

BOR1 の5′-UTRには四つの upstream open reading frame (uORF) が含まれる。uORFとは5′-UTRに含まれるORFを指し、しばしば翻訳装置であるリボソームを解離または停滞させることで下流のORFの翻訳を抑制する。そのため、uORFの存在が高濃度ホウ素条件で翻訳を抑制していると予想した。

BOR1 5′-UTRの翻訳制御に関わる配列を決定するため、配列の欠損または点変異を導入した変異型5′-UTRシリーズを作製し、シロイヌナズナの培養細胞と形質転換植物体でレポーターアッセイを行った。四つ全てのuORFを破壊した場合、ホウ素濃度依存的な発現パターンが失われたことから、*BOR1* 5′-UTRによるホウ素濃度依存的な発現抑制にuORFが必要であることが示された。また、いずれのuORFも単独では野生型5′-UTRと同程度の発現抑制を誘導しなかったが、2、3、4番目の三つのuORFを同時に持つコンストラクトでは野生型と変わらないホウ素濃度依存的な発現パターンが観察され、これら三つのuORFの存在がホウ素濃度依存的な発現抑制に十分であることが示された。

uORFによるホウ素濃度依存的な翻訳抑制の分子機構を明らかにするため、高濃度ホウ素条件における(i)リボソームの停滞、(ii) uORFの翻訳の上昇、(iii) uORF翻訳後の再翻訳頻度の変化、の三つの仮説を、リボソームの挙動を調べるトープリント試験と変異型*BOR1* 5′-UTRを用いたレポーターアッセイで検証した。その結果、(iii) uORF翻訳後の再翻訳が低濃度ホウ素条件における*BOR1*のORFの翻訳に必要であり、高濃度ホウ素条件において再翻訳の頻度が低下することが示唆された。

異なる植物の*BOR1*相同遺伝子の5′-UTRにはuORFが複数存在することから、ここで示したuORFを介したホウ素濃度依存的な翻訳制御機構が幅広い植物種に保存されていると考察された。

【2. ホウ素濃度依存的な発現制御の生理的意義】

BOR1 の選択的タンパク質分解と翻訳制御の二つの転写後制御を区別し、それぞれの生理的な意義を解明するため、いずれか一方の制御または両方の制御を失った*BOR1-GFP*を発現

する形質転換体を作製した。翻訳制御は配列欠損型の5′-UTRを用いることで、分解制御は制御に必要なリジン残基をアラニンに置換することで破壊した。

二つの転写後制御のホウ素濃度依存性を調べるため、これらの形質転換体を異なるホウ素濃度で生育させ、根におけるBOR1-GFPタンパク質の蓄積をウェスタンブロットで検出した。両方の制御を失った植物体ではBOR1-GFPはホウ素濃度に関わらず常に蓄積し、*BOR1*の発現を高ホウ素濃度で減少させる機構が本コンストラクトではこの二つの制御のみであることが示された。また、いずれか一方の制御のみを持つ植物体における観察から、分解制御が通常ホウ素条件（100 μM）以上で誘導されることに対し、翻訳制御は通常ホウ素条件では誘導されず高濃度ホウ素条件（1 mM）で誘導され、二つの制御が異なるホウ素濃度依存性を持つことを明らかにした。

また、二つの転写後制御の時間依存性を調べるため、制御を失った形質転換体を低濃度ホウ素条件から高濃度ホウ素条件に移植し、BOR1-GFPの蛍光シグナルの減少を経時的に観察した。分解制御を持つ植物体では過去の報告と一致して5時間以内に蛍光シグナルが減少した。一方で、翻訳制御のみを持つ植物体ではより緩やかな減少が観察された。

二つの制御の植物の生存における意義を調べるため、異なるホウ素濃度条件で水耕栽培を行った。高濃度ホウ素条件において、分解制御を失った植物体で生育阻害が観察された。ここで、分解制御のみを失った植物体と比べて両方の制御を失った植物体がより高濃度のホウ素を地上部に蓄積し、著しい生育阻害を示した。これは翻訳制御の寄与を示すと考えられる。よって、分解制御と翻訳制御の両方が高ホウ素濃度条件での過剰なホウ素の取り込みを防ぐ上で重要であることが示された。

以上の結果から、*BOR1* の二段階の制御は、通常ホウ素条件においては迅速な輸送の制御のためにタンパク質分解での制御を行い、より高濃度のホウ素過剰条件下では翻訳制御によりタンパク質の合成を抑制するという効率的な制御であると考察された。

【結論】

本学位論文で私は、植物が幅広いホウ素環境に適応するために濃度依存的、時間依存的に異なる二段階の発現制御機構を用いてホウ酸輸送体の量を調節することを明らかにした。これは植物が環境適応のために無機栄養輸送の緻密な調節機構を獲得してきたことを示す一例

である。また、今までに植物の無機栄養輸送体の翻訳段階での発現制御はほとんど報告がなく、本研究は植物の無機栄養環境への適応に関して新たな知見を与えるものである。

List of abbreviations

bp	base pair(s)
d	day(s)
DNase	deoxyribonuclease
h	hour(s)
kD	kilo dalton
Luc	firefly (*Photinus pyralis*) luciferase
ELuc(PEST)	Emerald luciferase fused to PEST sequence
min	minuite(s)
mRNA	messenger ribonucleic acid
nt	nucleotide(s)
NLuc	NanoLuc
Pro35S	cauliflower mosaic virus 35S RNA promoter
RG-II	rhamnogalacturonan II
RLuc	sea pansy (*Renilla reniformis*) luciferase
RNase	ribonuclease
tNOS	nopaline synthase (NOS) terminator
UTR	untranslated region

Introduction

For sessile plants, adaptation to soil environment is a crucial problem. One important factor in soil environment is a condition of mineral nutrients. The present study focuses on plant's adaptation to boron (B) environment.

Regulation of nutrient uptake in plants

Mineral environment for plants

Minerals are major determinants of plant growth and fertility in nature and agriculture. Plants require 17 essential elements to complete their life cycle; depletion of these elements causes various disorders of growth and development. Plants take up 14 of the 17 elements from the soil: nitrogen (N), phosphorus (P), potassium (K), sulfur (S), calcium (Ca), magnesium (Mg), iron (Fe), manganese (Mn), copper (Cu), zinc (Zn), molybdenum (Mo), boron (B), chloride (Cl), and nickel (Ni) (Marschner 2012).

Plants can take up these minerals only as soluble forms, such as ions in soil solutions. Nutrient solubility depends on the chemical form of each nutrient, which is affected by environmental factors, including water content, pH, redox potential, abundance of organic matter, and microorganisms in soils (Marschner 2012). Since local soil environments are heterogeneous and change readily, soil nutrient availability is highly variable and often limited. In addition, nutrient mobility in soils is influenced by their chemical form and environmental factors. The accessibility of nutrients with limited mobility, including P and Fe, in soil is restricted to roots near the location of the nutrient. The mobility of elements relatively mobile in soil depends on the water conditions. These differences, including soil nutrient mobility, result in different spatial distributions (Jobbagy and Jackson 2001). Therefore, plants must cope with the uneven spatial distributions and temporal changes of nutrients to optimize nutrient acquisition throughout their life cycle.

Modulation of root morphology

One useful strategy for efficient nutrient uptake is modulation of the root system architecture according to the nutrient conditions. Nutrient concentrations affect the length, number, angle and diameters of the

primary roots and lateral roots, and root hair development. These developmental changes result in nutrient-dependent root-system patterns. For example, under P starvation, primary root elongation is inhibited, while lateral root formation is enhanced concomitantly (Williamson et al., 2001; Lopez-Bucio et al., 2002), resulting in the formation of a shallow root morphology and increased root surface area. Phosphate tends to accumulate in the topsoil layer (as it readily binds to soil organic matter) where it is immobilized (Jobbagy and Jackson 2001). Thus, belowground morphological responses of plants to P starvation likely contribute to efficient acquisition of phosphate by exposing a large root surface area to P, as supported by experimental data and mathematical models (Ge et al., 2000; Rubio et al., 2003; Heppell et al., 2014). In contrast, for water-soluble nutrients such as nitrate and sulfate, which are readily leached to deeper soil layers, root development towards lower layers is preferred.

Changes in whole root architecture in response to P and N conditions have been intently characterized. However, the effects of other nutrients on root architecture have not been well described. Gruber et al. (2013) reported the profiles of root system architecture in *Arabidopsis thaliana* grown under nine macro- and micronutrient deficiencies (P, N, Ca, K, Mg, S, Fe, Mn, and B). The root morphology showed unique patterns under deficiency of each single nutrient. It is not yet clear how these architectural changes benefit the plants in terms of soil nutrient acquisition; however, it seems that plants alters its root system architecture in a nutrient-specific manner.

Regulation of nutrient transporter activities

Another major strategy is modulation of transport activity within and among plant organs. Nutrient transporters regulate nutrient uptake into root cells and subsequent translocation within the plant body. Transport molecules for each essential nutrient have been identified in *A. thaliana*. Increasing evidence indicates that plants have evolved diverse transporters with distinct substrate specificities, transport affinities, cell-type expression, and subcellular localization to ensure appropriate flux and compartmentalization of each transport process within the plant body/cell.

Many examples of the nutrient-dependent regulation of transporter expression are available. Nutrient conditions strictly regulate transporter gene expression at both the transcriptional and post-transcriptional levels. Transporters also undergo post-translational modification to control transport

activities. This regulation at multiple steps benefits nutrient homeostasis under a wide range of nutrient conditions. Although transcriptional regulation of such transporters has been studied intensively, there are few reports of post-transcriptional regulation, especially translational regulation.

Boron in plants

Chemical characteristics

Boron is one of micronutrients, and its available form for plant is boric acid. Boric acid is a weak Lewis acid with p*K*a 9.24 $B(OH)_3 + H_2O = B(OH)_4^- + H^+$. Under near-neutral fluids in most biological situations, B mainly exists as boric acid [$B(OH)_3$] and partly as borate anion [$B(OH)_4^-$]. Boric acid and borate have capacity to form complexes with compounds containing *cis*-hydroxyls, such as furanose, through forming diester with the two pairs of hydroxyl moieties (Bolanos et al., 2004; Marschner 2012).

In soil, boric acid is highly mobile and easily leached out by rainfalls. Besides, drying up of topsoil water results in accumulation of boric acid. These factors possibly changes local B condition in soil, in addition to ecological or biological factors (such as decomposition of organic matters).

Essentiality of boron

The essentiality of B in plants was first demonstrated in 1923 by Warington (Marschner, 2012). Under B starvation, plants exhibit various symptoms such as inhibition of leaf expansion and root elongation, and loss of fertilities. In plant cells, B is predominantly distributed to cell wall, where it crosslinks pectic polysaccharide rhamnogalacturonan-II (RG-II) (Funakawa and Miwa, 2015). To date, this is the only established physiological function of B among organisms. RG-II is a complex polysaccharide composed of 12 kinds of monosaccharides including apiose, which was demonstrated as the target site of B binding. Thus, borate contributes to formation of cell wall network.

The necessity of RG-II crosslinking by borate has been confirmed in *A. thaliana* mutant *mur1* (O'Neill et al., 2001). *mur1* contained lower level of borate cross-linked RG-II in shoot, because of altered RG-II structure. This mutant shows dwarfed phenotype with less leaf expansion in normal B nutrient condition. Application of high concentration of B recovered both RG-II cross-linking rate and

the dwarfed phenotype, suggesting that the borate cross-linked RG-II is required for normal growth of plants.

Boron toxicity

Excess B is toxic to organisms including plants. Typical symptoms of B toxicity are reduction of shoot growth, chlorosis of mature leaves, inhibition of root development and infertilities. Although the molecular target of B in B toxicity is still unclear, biological processes affected by toxic level of B have been investigated. Sakamoto et al. took a forward genetics approach to reveal the mechanism of B toxicity (Sakamoto et al., 2011). They obtained *A. thaliana* mutants which are hypersensitive to high B. The causal genes encoded subunits of condensin II complex, which is involved in maintenance of chromosome structure. Further, DNA damage was observed in roots exposed to excess B, and treatment by reagents which induce DNA damage mimicked effects of B toxicity. This study suggests that DNA damage is one of the causes of B toxicity

Boron Transporters

Boron transporters for efficient uptake

To cope with the narrow optimum range of B concentration, plants use different types of B transporters (Yoshinari and Takano, 2017). Under B deprivation, the *NODULIN 26-LIKE INTRINSIC PROTEIN 5;1* (*NIP5;1*) and *BOR1* genes are expressed in roots to support the effective translocation of B in *A. thaliana*.

NIP5;1 is a member of the major intrinsic protein family, which facilitates diffusion of water and/or small uncharged molecules (Takano et al., 2006). NIP5;1 is mainly located in soil-facing side of plasma membrane of outermost cell layers in roots, and thus contributes to uptake of B from soil to root cells (Takano et al., 2010). A recent study demonstrated the mechanism and the importance of the soil-side localization of NIP5;1 (Wang et al., 2017). Polar localization of NIP5;1 is established by endocytosis after phosphorylation at the conserved motif of NIP5;1. Transgenic lines with disruption of the motif in NIP5;1 transported lower amounts of B into shoot and exhibited growth reduction under low B, suggesting the importance of the soil-side localization on efficient B uptake.

BOR1 is an efflux borate transporter homologous to anion exchangers, and is expressed in various cell types including epidermis and endodermis. It exports borate out of cells toward the xylem and contributes to the translocation of B from roots to shoots (Takano et al., 2002; Takano et al., 2010). While NIP5;1 is located in soil-side of plasma membrane, BOR1 is located in stele-side of plasma membrane. This localization was found to be established by removal of BOR1 from soil-side plasma membrane through endocytosis by clathrin and DRP1 (Yoshinari et al., 2016). *BOR2*, the closest paralog of *BOR1*, also contributes to plant adaptation to B depletion, through facilitating crosslink of RG-II under low B conditions (Miwa et al., 2013).

Transporters for exclusion of boron

As boric acid readily permeates cell membranes, plants need to exclude B under high B concentrations to prevent excess accumulation of B in its body. Another *BOR1* paralog, *BOR4*, functions in the exclusion of borate in roots in *A. thaliana* (Miwa et al., 2014). BOR4 is localized to soil-facing side of plasma membrane in epidermal cells, probably to export B from root to soil (Miwa et al., 2007).

Orthologous genes of *BOR*s and *NIP5;1* are identified or predicted in many plant species: BORs were found in rice (*Oriza sativa*), wheat (*Triticum aestivum*), barley (*Hordeum vulgare*), maize (*Zea mays*), grapevine (*Vitis vinifera*), citrus (*Citrus macrophylla*), a lycophyte (*Selaginella moellendorffii*) and a bryophyte (*Physcomitrella patens*) (Nakagawa et al., 2007; Reid, 2007; Sutton et al., 2007; Perez-Castro et al., 2012; Cañon et al., 2013; Leaungthitikanchana et al., 2013; Chatterjee et al., 2014; Wakuta et al., 2015), and NIPs transporting B were found in rice and maize (Durbak et al., 2014; Hanaoka et al., 2014). These B transporters coordinately control B transport in plant bodies in response to external B conditions.

Expression regulations of boron transporters

Expression regulation of *NIP5;1* and *BOR1*

Recent studies have revealed several mechanisms of B-dependent regulation of B transporter gene expression. Under sufficient B, expression of *NIP5;1* is downregulated via post-transcriptional

regulation (Tanaka et al., 2011). During translation, ribosomes are stalled in its 5′-untranslated region (UTR), which enhances the destabilization of *NIP5;1* mRNA (Tanaka et al., 2016). Thus, *NIP5;1* mRNA is present at lower levels under sufficient B conditions than under low B conditions.

In contrast to *NIP5;1*, *BOR1* expression is not altered at the mRNA level, but is regulated at the protein level (Takano et al., 2005). Under B sufficiency (100 μM boric acid in the medium), BOR1 undergoes ubiquitination followed by endocytic protein degradation (Takano et al., 2005; Kasai et al., 2011). Lysine-590 is required for this ubiquitination (Kasai et al., 2011), and three tyrosine motifs and a di-leucine motif have been shown to be essential for post-endocytic trafficking (Takano et al., 2010; Wakuta et al., 2015). Replacement of these amino acid residues effectively inhibits the reduction of BOR1 under sufficient B concentrations. However, it has been demonstrated that even if the tyrosine motifs are disrupted, BOR1 accumulation decreases when treated with toxic concentrations of B (e.g., 1,000 and 3,000 μM) for a long period (Takano et al., 2010). This suggests the presence of another *BOR1* regulatory mechanism that is induced by higher B concentrations.

The aim of the present thesis is to reveal the mechanism that regulates B-dependent *BOR1* expression independent of selective protein degradation, and the biological significance of the two regulatory mechanisms. In chapter1, B-dependent translational suppression mediated by the *BOR1* 5′-UTR is described. In chapter2, the biological roles of the translational suppression and the selective protein degradation are shown. Translational suppression of *BOR1* was induced under higher B concentrations than those required to induce BOR1 degradation, thus revealing that these two regulatory mechanisms depend on different B concentrations. In addition, it is demonstrated that this post-transcriptional regulation of *BOR1* expression contributes to plant survival under high B conditions by avoiding excess transport of B.

Chapter1 –Molecular mechanisms of boron-dependent translational suppression-

In addition to the selective protein degradation under sufficient B condition, the presence of additional B-dependent expression regulation has been suggested. However, the regulatory mechanism had not been dissected. In this chapter, the presence of B-dependent translational regulation by *BOR1* 5´-UTR is revealed and the detailed mechanism is investigated.

1.1 Materials and Methods

1.1.1 Plant Growth and Transformation

Arabidopsis thaliana (L.) Heynh. ecotype Columbia (Col-0) was used as a wild-type strain. Col-0 and *bor1-1*, a loss-of-function mutant of *BOR1*, were derived from the laboratory stock. Plants were grown in solid or liquid media (Fujiwara et al., 1992) in which B concentration was adjusted with boric acid. Boric acid concentrations in media were set in the range where Col-0 plant growth was not impaired. The boric acid concentration for toxic-B conditions in hydroponic was set lower than solid medium system (~mM levels) due to high transpiration stream. Solid media additionally contained 1% (w/v) sucrose and 1% (w/v) gellan gum (Wako Pure Chemicals). Plants were incubated at 22°C in growth chamber. Light conditions were a 16 h light / 8 h dark cycle.

For transformation, Col-0 was used as a background plant for pIA and pTF series. Transformation was conducted with *Agrobacterium tumefaciens* strain GV3101 (C58C1Rif^r) pMP90 (Gm^r), according to floral dip method. Transformants were selected on solid media containing 1% (w/v) sucrose, 0.15% (w/v) gellan gum and hygromycin B (20 mg L^{-1}) for pIA series, and 1% (w/v) sucrose, 0.8% (w/v) agar and kanamycin (50 mg L^{-1}) for pTF series.

1.1.2 Plasmid Construction

Plasmids used in this study and primers for construction are listed in Table 1, and the sequences of the primers are shown in Table 2. Plasmids carrying point-mutated *BOR1* 5′-UTR are listed in Table 3. Plasmid construction was performed as follows.

For GUS assay, pTF462 (UTR^{WT}) and pTF463 ($UTR^{356-251}$) were generated by Dr. Toru Fujiwara. GUS ORF was amplified with primers A1 and A2 using pBI101.1 (Jefferson et al., 1987) as template. The six nucleotides ATGGTA encoding Met-Val, were inserted at the 5′ end of the original GUS ORF to generate an *Nco*I site. The PCR fragment was digested with *Sac*I and *Bam*HI, and inserted into pTF377 containing CaMV 35S promoter and NOS terminator in pUC119, resulting in pTF452 (Pro35S: GUS-tNOS in pUC119). *BOR1* promoter fragments UTR^{WT} and $UTR^{356-251}$ were amplified with primer sets A3-A5 and A3-A4, respectively. The resultant fragments were digested with *Bam*HI and *Nco*I, and cloned into pTF367 derived from pTH2 (Niwa, 2003), resulting in pTF439 and pTF440. In the plasmids, the last two or four nucleotides of *BOR1* promoter regions were substituted during the process of construction. *Bam*HI-*Nco*I vector fragment from pTF367 is identical to the *Bam*HI-*Nco*I vector fragment from pTH2. To replace CaMV 35S promoter of pTF452 with *BOR1* promoter, *Sph*I-*Nco*I fragments of pTF439 and pTF440 were inserted into *Sph*I-*Nco*I digested pTF452, to generate pTF453 and pTF454 carrying ProBOR1:GUS-tNOS in pUC119. pTF462 (UTR^{WT}) and pTF463 ($UTR^{356-251}$) were generated by inserting *Bam*HI-*Eco*RI fragment from pTF453 and pTF454, respectively, into the corresponding sites of pBIN19 (Bevan, 1984).

For transient assay in cultured cells, Pro35S-tNOS in pUC19 was used as a basal structure. For ΔUTR (pIA1), ELuc(PEST) region was amplified with primers, to insert *Xba*I and *Kpn*I sites to 5′-end and *Sac*I site to 3′-end. The resultant fragment was cloned to pUC19-Pro35S-Renilla luciferase (RLuc)-tNOS (pKM75, Tanaka et al., 2016) between *Xba*I and *Sac*I to replace RLuc with ELuc(PEST). For UTR^{WT} (pIA2) and CIPK1UTR (pIA13), *BOR1* or *CIPK1* 5′-UTR sequence were amplified using total cDNA as template. The fragments were cloned into pIA1 between *Xba*I and *Kpn*I site, resulting in pIA2 and pIA13. In UTR^{WT}, the downstream 9 nt of the 5′-UTR were replaced to linker sequence, so the construct actually harbors 347 nt (-356 to -10) of the 5′-UTR. For $UTR^{356-251}$ (pIA22), *BOR1* 5′-UTR was amplified with pIA2 as template, and the fragment was inserted into pIA2 between *Xba*I and *Kpn*I site. The truncated *BOR1* 5′-UTR series were constructed as the same procedure with pIA22, using corresponding primers. Resulting plasmids were named as UTR^{356-97} (pIA6), $UTR^{356-136}$ (pIA19), $UTR^{356-235}$ (pIA20), UTR^{253-10} (pIA11), UTR^{239-10} (pIA17), UTR^{140-10} (pIA18) and UTR^{96-10} (pIA71).

For generating transgenic plants carrying *BOR1* 5′-UTR:ELuc(PEST), plasmids were constructed with pMDC99 as backbone plasmid. CaMV 35S RNA promoter fragment in pIA1 were digested and inserted into pMDC99 with *Hin*dIII and *Xba*I. In the plasmid, ELuc(PEST) with/without *BOR1* 5′-UTR was further inserted with *Xba*I and *Eco*RI, resulting in pIA35 and pIA34, respectively. To generate point-mutation series of *BOR1* 5′-UTR, amplified products were first cloned in in pSP64 poly(A) vector (Promega). Each point mutation was introduced by primers 27-28 for uORF1, 1B-1C for uORF2, 2B-2C for uORF3, 3B-3C for uORF4, 4B-4C for uORF3 and 4, and resulting plasmids are listed in Table 3. The point mutated 5′-UTRs were cloned into pIA35 with *Xba*I and *Kpn*I, resulting in No_uORF (pIA57), uORF1_single (pIA53), uORF2+3+4 (pIA52), uORF2_single (pIA54), uORF3_single (pIA55), uORF4_single (pIA56) and uORF3+4 (pIA58).

For *in vitro* translation, UTR^{WT} (pIA24) and $UTR^{356\text{-}251}$ (pIA28) were constructed. pMI21 (Chiba et al., 2003) was used as backbone plasmid, carrying a *luc*+ gene in pSP64 poly(A) vector (Promega). Upstream sequence of *luc*+ was replaced to native or truncated *BOR1* 5′-UTR derived from pIA2 and pIA22 by *Xba*I and *Nco*I. No_uORF (pIA50) and uORF2+3+4 (pIA36) were generated as products of point-mutation series shown in Table 3.

To use Nluc(PEST) reporter, the plasmid Pro35S:NLuc(PEST)-tNOS in pUC19 (pTI01) was generated. NLuc(PEST) fragment was amplified by primers A6 and A7, with pNL1.2[NlucP] (Promega) as template to introduce *Xba*I, start codon and *Sal*I site at 5′-end, and *Sac*I site at 3′-end. The amplified fragment was cloned into pBI221 (Clontech) with *Xba*I and *Sac*I to replace GUS with Nluc(PEST), resulting in pTI01.

For the plasmids containing luciferase-fused uORFs, uORF2 fusion (pIA65), uORF3 fusion (pIA62), uORF4 fusion (pIA63) and uORF3+4 fusion (pIA64), point-mutated 5′-UTR were amplified from the templates pIA36, pIA47, pIA48 and pIA36, respectively. pIA47 and pIA48 are shown in Table 3. The amplified fragments were ligated into pTI01 in *Sal*I and *Xba*I.

For the plasmids for reinitiation test, uORF2+3+4 (pIA59) and uORF2+3+4_del (pIA60), uORF1-disrupted 5′-UTR was amplified from uORF2+3+4-FLuc (pIA36). The resultant fragments were inserted into pTI01 by *Sal*I and *Xba*I digestion. To synthesize uORF2+3+4_long (pIA61), three DNA

fragments were amplified with primer sets 450-453, 454-455, and 456-451, introducing two point-mutations in the 5′-UTR. The resultant fragments were mixed to connect each other in the second PCR, using primers 450 and 451, to generate mutated 5′-UTR fragment. The amplified fragment was inserted into pTI01 by *Sal*I and *Xba*I.

1.1.3 mRNA Quantification

Eight-day-old plants grown under 30 μM boric acid were transferred to the solid media containing 0.1, 30 or 3,000 μM of boric acid and were then incubated for 3 d. Total RNA extraction from roots by RNeasy Plant Mini kit (QIAGEN), reverse transcription and quantitative real-time PCR were performed as described (Miwa et al., 2014). The sequence of primers for *BOR1* and *elongation factor 1α* (*EF1α*) were described in Takano et al. (2005), and the primers for *GUS* and *β-tublin* were in Miwa et al. (2014). *BOR1* and *GUS* transcript levels were standardized to the levels of *β-tublin* and *EF1α*, respectively. The values of *BOR1*/*β-tublin* are those relative to the mean value at 30 μM boric acid, which was defined as 1.

1.1.4 Measurement of GUS Activity

Plants carrying *ProBOR1*:(*BOR1* 5′-UTR):*GUS* were first grown under 30 μM boric acid for 8–9 d and were exposed to 0.3 or 3,000 μM boric acid for 3 d. The bulk of 30–40 T2 plants in one independent line were harvested as one sample. Protein extraction from roots, measurement of GUS activity and total protein concentration by Bradford assay were conducted as described (Miwa et al., 2014). Relative values of *GUS* mRNA (*GUS*/*EF1α*) and GUS activity (production of 4-MU mmol g^{-1} protein min^{-1}) under 3,000 μM were determined when the values at 0.3μM boric acid was set to 1 in each of the transgenic lines, respectively.

1.1.5 Transient Expression Analysis in Cultured *A. thaliana* Cells

The transient expression analysis was basically performed as described in Ebina et al. (2015). The test plasmids containing ELuc(PEST) reporter were co-transfected with the internal control plasmid Pro35S:Renilla luciferase (RLuc) (pKM75, Tanaka et al., 2016). When NLuc(PEST) was used in the

test plasmids, Pro35S:ELuc(PEST) (pIA1) was used as a control plasmid. Protoplasts of cultured *A. thaliana* cells MM2d (Menges and Murray, 2002) were transformed with plasmid DNAs by electroporation, and incubated under 1, 500 or 750 μM of boric acid. For preparation of protoplasts, MM2d cells in log phase was collected by centrifugation and then washed by 0.4 M mannitol solution. The cells were suspended in enzyme solution (PCM medium containing 1% (w/v) cellulase RS (YAKULT), 0.1% (w/v) pectolyase Y-23 (KYOWA CHEMICALS)) and incubated for 3 h at 26°C under darkness with gentle shaking. PCM medium is LS medium containing 0.4 M mannitol. The protoplasts were collected by centrifugation and washed by wash buffer (0.4 M mannitol, 5 mM $CaCl_2$ and 12.5 mM sodium acetate (pH 5.8)). Protoplasts were suspended in 0.4 M mannitol.

DNA solution, containing 10 μg of test plasmids and 5 μg of control plasmid, was mixed with 2 x 10^6 protoplasts in 500 μL of electroporation buffer (5 mM 2-morpholinoethanesulfonic acid, 70 mM potassium chloride and 0.3 M mannitol, pH 5.8). Samples were subjected to electroporation by ECM630 (BTM), at 190 V, capacitance 100 μF and resistance 475Ω. Protoplasts were incubated at 25°C for 5 min. Protoplasts were collected and suspended in 1.6 ml of PCM medium (prepared without boric acid), and dispensed to 3 equivalent portions (500 μL each). 500 μL of PCM medium, containing different concentrations of boric acid, was added to protoplasts to expose the cells under 1, 500 and 750 μM of boric acid. Protoplasts were incubated at 22°C for 40–45 h under continuous darkness. After incubation, the protoplasts were homogenized in 100 μL of protein extraction solution (100 mM sodium phosphate (pH 7) and 5 mM dithiothreitol (DTT)), and cell debris were removed by centrifugation. The extracts were subjected to luciferase assay. To measure ELuc and RLuc activities, PicaGene Dual Sea Pansy Luminescence kit (TOYO INK) was used. For combination of NLuc and ELuc, Nano-Glo® Luciferase Assay System (Promega) and PicaGene Luminescence kit (TOYO INK) was used to measure each activity separately.

1.1.6 Luciferase Assay in Transgenic Plants

T3 homozygous plants carrying *ProBOR1*:(*BOR1 5′*-UTR):*ELuc(PEST)* were continuously grown on solid medium containing 0.3, 500 or 1,000 μM of boric acid for 12 d. Roots were harvested from 18–20

plants from one independent line as one sample and homogenized in protein extraction buffer (50 mM sodium phosphate (pH 7), 5 mM DTT and 2 mM EDTA). Cell debris were removed by centrifugation and the supernatant was subjected to luciferase assay. ELuc activities were measured by PicaGene Luminescence kit (TOYO INK). To normalize the ELuc activity, total protein concentration were measured by Bradford assay using Quick Start™ Bradford Protein Assay (BIO-RAD). Reporter activities at 500 and 1,000 μM of each independent line were calculated as relative value when the value at 0.3 μM was set to 1.

1.1.7 *In Vitro* Translation and Toeprint Assay

For *in vitro* translation, RNAs carrying poly(A) sequence were synthesized in *in vitro* transcription. Plasmids UTR^{WT} (pIA24), $UTR^{356\text{-}251}$ (pIA28), No_uORF (pIA50) and uORF2+3+4 (pIA36) were used. For control (*RLuc-*A_{30}), pMI27 (Chiba et al., 2003) carrying a RLuc gene in pSP64 poly(A) vector was used. Plasmids were linearized by digestion with *Eco*RI. Linearized DNA was purified by FastGeneTM Gel/PCR Extraction kit (NIPPON Genetics) and dissolved in RNase/DNase free water. For each construct, 1 μg of DNA was subjected to *in vitro* transcription by AmpliCap™ SP6 High Yield Message Maker kit (CellScript) according to the manufacture's instruction. Synthesized RNA was purified by RNeasy Plant Mini kit (QIAGEN) and dissolved in RNase-free water. Then, poly(A)-RNA was isolated by binding to oligo(dT) beads using GenElute mRNA Miniprep Kit (Sigma-Aldrich).

Synthesized RNAs, test RNA (*BOR1 5'-UTR-LUC-*A_{30}) and control RNA (*RLuc-*A_{30}), were subjected to *in vitro* translation under various boric acid concentrations. *In vitro* translation was carried out following the protocol of WGE (Promega). WGE, amino acid solution and RNase inhibitor (RNasin; Promega) was mixed on ice and aliquoted. Filtered boric acid was added to 1, 10, 100, 250, 500 and 1000 μM as final concentration. The boric acid concentrations were set in the range where control reporter activities were not lowered. Synthesized RNAs, 20 fmol of test RNA and 2 fmol of the control RNA was added. After incubation for 2 h at 25°C, samples were transferred on ice and diluted by 50-fold by ice cold water. The diluted samples were subjected to FLuc-RLuc dual luciferase assay using PicaGene Dual Sea Pansy Luminescence kit (TOYO INK).

Toeprint assay was carried out as described in Hayashi et al. (2017). Oligonucleotide primer 416 (Table 2) was labeled at its 5′ terminus with T4 polynucleotide kinase (Takara) and [γ-^{32}P] ATP (110 TBq/mmol; Perkin Elmer). *In vitro* translation of 200 fmol synthetic RNA (*BOR1 5′ -UTR-LUC-A$_{30}$*) was performed with the addition of 0 or 1,000 μM boric acid and 0 or 2 mM of hygromycin B as final concentration. Translation samples were subjected to reverse transcription by SuperScript® III First-Strand Synthesis System (ThermoFisher) using the ^{32}P-labeled primer. Reverse transcription samples were separated by electrophoresis on an 8% (w/v) polyacrylamide/7 M urea sequence gel. DNA sequence ladder was prepared with pIA50 (No_uORF) as a template.

1.1.8 Statistical Analyses

Following statistical analyses were conducted by R software: Student's *t*-test for *GUS* mRNA, GUS activity and reporter activity measurements (Figs. 2, 3, 6), Dunnett's test after ANOVA for reporter activity measurements (Fig. 4).

1.1.9 Accession Numbers

Arabidopsis Genome Initiative locus identifiers for the genes in this article are as follows: *BOR1* (At2g47160), *NIP5;1* (At4g10380), *BOR2* (At3g62270), *BOR4* (At1g15460), *CIPK1* (At3g17510). *BOR1* cDNA sequence data can be found in the GenBank/EMBL databases under accession number BT000732.

1.2 Results

1.2.1 *BOR1* 5´-UTR Is Required for the Translational Suppression of the Main Open Reading Frame (ORF) under High B Conditions

To examine the mechanism of the downregulation of *BOR1* expression in the presence of high B concentrations (> 100 μM), mRNA accumulation was quantified in roots under low (0.1 μM), sufficient (30 μM), and toxic (3,000 μM) concentrations of B as boric acid (Fig. 1). The experiments in Figs. 1 and 2 were performed by Dr. Kyoko Miwa. It has been reported that low B treatment does not affect *BOR1* mRNA accumulation (Takano et al., 2005). In this study, even under toxic B concentrations, *BOR1* mRNA accumulation was not significantly decreased. This suggested that the downregulation mechanism at high B concentrations did not likely involve transcription or mRNA degradation.

To clarify this post-transcriptional mechanism, the effect of B on the translation of *BOR1* mRNA was examined (Fig. 2). In general, 5´-UTRs have an important role in translational regulation (Hinnebusch et al., 2016). *BOR1* 5´-UTR is defined as 356 nt (Fig. 3A) based on experimentally obtained full-length cDNA sequences (Seki et al., 2002). First, the contribution of the 5´-UTR to B-dependent translation was investigated in transgenic *A. thaliana* carrying a *ProBOR1:(BOR1 5´-UTR):GUS* construct under low and toxic B conditions (0.3 and 3,000 μM boric acid, respectively). In the transgenic line carrying the wild-type 5´-UTR (UTR^{WT}), β-glucuronidase (GUS) activity decreased to 40% under the toxic B concentration compared to that under the low B concentration (Fig. 2A), whereas removal of 250 nt on the 3´ end of the 5´-UTR ($UTR^{356-251}$) resulted in the loss of the B-dependent reduction in GUS activity (Fig. 2A). *GUS* mRNA accumulation was not affected by B concentration (Fig. 2B) in either construct. These results suggested that the 5´-UTR was involved in translational suppression under toxic B conditions and that 250 nt in the 3´ portion were required for this regulation.

BOR1 5′-UTR Is Sufficient for B-Dependent Gene Expression

To determine whether the *BOR1* 5′-UTR can confer B-dependent regulation, we performed an expression analysis with a constitutive cauliflower mosaic virus (CaMV) 35S RNA promoter. The *ELuc(PEST)* reporter gene fused to the *BOR1* 5′-UTR was transiently expressed in cultured *A. thaliana*

cells exposed to low (1 μM) and high (500 and 750 μM) concentrations of B as boric acid (Fig. 3B). The B concentrations used were in the range in which control reporter gene activity was not lowered. In the control construct without the 5′-UTR (ΔUTR), reporter activity did not change under different B concentrations, indicating that the enzymatic activity of ELuc(PEST) was not affected by B conditions. In the presence of the *BOR1* 5′-UTR (UTR^{WT}), reporter activity decreased with increasing B concentration. Consistent with the results *in planta* (Fig. 2A), the truncated 5′-UTR ($UTR^{356-251}$) did not induce B-dependent downregulation. This demonstrated that B-dependent gene expression mediated by the *BOR1* 5′-UTR occurred in the transient expression system in *A. thaliana* culture cells, and that this response was activated in the presence of 500 μM B in the medium. Furthermore, we analyzed the effect of the *CBL-INTERACTING PROTEIN KINASE 1* (*CIPK1*) 5′-UTR (CIPK1UTR), which is similar in length (294 nt) to the *BOR1* 5′-UTR, as an example of genes unrelated to B nutrition. Reporter gene activity with CIPK1UTR did not change significantly in response to different B concentrations. These results showed that the *BOR1* 5′-UTR sequence was sufficient for B-dependent gene expression, and that the downregulation was specific to the *BOR1* 5′-UTR.

1.2.2 Two Independent Regions in the *BOR1* 5´-UTR Induce B-Dependent Expression

The *BOR1* 5´-UTR harbors four short ORFs (Fig. 3A) called upstream ORFs (uORFs). The four uORFs were named uORF1 to uORF4 starting from the 5´ end. The uORF1 sequence is AUGUAA, a minimum ORF consisting of a start codon and stop codon as characterized in *NIP5;1* (Tanaka et al., 2016). uORF3 and 4 are in-frame ORFs, sharing the same stop codon and possessing one or both of two important nucleotides (A/G at –3, G at +4) in the Kozak consensus sequence for efficient translation (Kozak, 1986; Joshi et al., 1997; Sugio et al., 2010). In eukaryotes, uORFs are known to affect translation of the downstream ORF (Kozak, 1986; von Arnim et al., 2014; Hinnebusch et al., 2016).

Focusing on the presence of the uORFs, a series of truncated *BOR1* 5´-UTR fragments was constructed to identify the regions responsible for B-dependent expression (Fig. 3B). Portions of the 5´-UTR sequences were deleted from the 3´ end (referred to as UTR^{356-97}, $UTR^{356-136}$, $UTR^{356-235}$, and $UTR^{356-251}$) and from the 5´ end (UTR^{253-10}, UTR^{239-10}, UTR^{140-10}, and UTR^{96-10}). Since uORF3 and 4 are

in-frame, a construct that deleted only one of them was not created. The effects of the truncated series of 5´-UTRs were analyzed in cultured cells. The result of this experiment is partly shown in my master's thesis (2014).

The UTR^{WT} induced a reduction in the relative reporter activity with increasing B concentration, ultimately decreasing to 24% at 750 µM compared to 1 µM (Fig. 3B). B-dependent reductions of 51–65% were observed at 750 µM B in most of the 3´-deleted constructs, including $UTR^{356\text{-}97}$, $UTR^{356\text{-}136}$, and $UTR^{356\text{-}235}$, although the extent of the reduction was weaker compared to that of UTR^{WT}. However, the B-dependent reduction in reporter activity was lost in $UTR^{356\text{-}251}$. These results indicated that the 5´ portion of the 5´-UTR between –356 and –235, but not between –356 to –251, supported B-dependent downregulation. This implied that the *cis*-acting element required for the regulation possibly existed in the 122-nt region between –356 and –235, which included uORF1.

Furthermore, B-dependent expression was observed in the three 5´-end truncated constructs ($UTR^{253\text{-}10}$, $UTR^{239\text{-}10}$, and $UTR^{140\text{-}10}$), and the reporter activities were reduced to 25–39% at 750 µM. However, the B-dependent expression was not observed in $UTR^{96\text{-}10}$, which carried no uORF. The results showed that 131 nt in the 3´ portion of the 5´-UTR (–140 to –10) was sufficient for regulation, which included uORF3 and uORF4.

Since $UTR^{356\text{-}235}$ and $UTR^{140\text{-}10}$ do not overlap to each other, these results clearly suggested that there were at least two independent regions in the 5´-UTR that were responsible for B-dependent downregulation. The results also imply possible contribution of uORFs in suppression of basal expression level of a main ORF, as $UTR^{356\text{-}251}$ and $UTR^{96\text{-}10}$, which contained no uORF, showed higher reporter activities independent of the B conditions.

1.2.3 uORFs Are Necessary for B-Dependent Translation *in Planta*

To examine the involvement of uORFs in B-dependent expression, mutations were introduced to replace the start codons of the uORFs with an AAG sequence in various combinations (Fig. 4). Among the factors in the 5´-UTR structure that affect translation efficiency, the large mRNA secondary structure was unlikely to be required for B-dependent expression based on the results showing that two relatively

short regions, 122 nt in the 5′ portion of 5′-UTR and 131 nt in the 3′ portion of the 5′-UTR, independently regulated B-dependent expression (Fig. 3B). Moreover, the internal ribosome entry site (Hellen and Sarnow, 2001) was not predicted to be present in the corresponding nucleotides. Therefore, the effects of these mutations likely occurred through the disruption of the uORFs.

Transgenic plants carrying the series of constructs shown in Figure 4 were generated. Several independent lines were generated for each construct, and lines homozygous for transfer DNA insertion were established. The reporter activities in roots were determined in the transgenic plants grown under low (0.3 μM), high (500 μM), and toxic (1,000 μM) concentrations of B as boric acid. The relative reporter activities at 500 and 1,000 μM compared to that at 0.3 μM are shown for the respective independent transgenic lines.

In the wild-type 5′-UTR lines (UTR^{WT}), reporter activity was markedly decreased with increasing B concentration, while for the ΔUTR construct, no such reduction was observed. Since *ELuc(PEST)* mRNA accumulation was not affected by B concentration, these results indicated that the *BOR1* 5′-UTR was sufficient for B-dependent translation *in planta*, consistent with the observations in the transfection (or transient expression) experiments shown in Figure 3B. Disruption of all four uORFs by the AUG-to-AAG mutations (No_uORF) resulted in the complete loss of B-dependent suppression of reporter expression. This result demonstrated that *BOR1* uORFs were necessary to elicit a response to B concentration.

1.2.4 Multiple uORFs Control B-Dependent Translation

BOR1 uORF1 (AUGUAA) is a minimum ORF, which has been reported to promote ribosome stalling under high B concentrations, leading to the suppression of main ORF expression in *NIP5;1* (Tanaka et al., 2016). To distinguish the effect of uORF1 from the other uORFs, mutated 5′-UTRs carrying only uORF1 (uORF1_single) or the other three uORFs (uORF2+3+4) were compared.

Unexpectedly, the extent of B-dependent suppression of the reporter expression was markedly weaker in the uORF1_single plants than in the UTR^{WT} plants. The mean value of the reporter activity in the UTR^{WT} plants was 0.17 at 1,000 μM B when the reporter activity at 0.3 μM was set to 1, while the

uORF1_single plants showed only a modest reduction, reaching 0.65 at 1,000 μM B. Meanwhile, the uORF2+3+4 plants, with a reporter activity of 0.14 at 1,000 μM B, induced B-dependent regulation comparable to the level observed in the UTR^{WT} plants. The occurrence of the B response in the uORF1_single and uORF2+3+4 plants was in agreement with the observation that two independent regions caused B-dependent suppression in cultured cells, as shown in Figure 3. As observed *in planta*, the results indicated that uORF1 (AUGUAA) was functional but not necessarily required, and that the other three uORFs were the pivotal *cis*-element for B-dependent regulation of translation. This demonstrates the presence of a regulation mechanism that differs from that present in *NIP5;1*, which requires AUGUAA for regulation.

Next, we examined the effects of uORF2, 3, and 4 independently using the constructs uORF2_single, uORF3_single, and uORF4_single. The presence of uORF2 alone did not induce B-dependent expression suppression, similar to the ΔUTR and No_uORF constructs. In contrast, uORF3_single and uORF4_single induced B-dependent expression, although the extent of the suppression was less than that of UTR^{WT}. The mean of suppression values of uORF3_single and uORF4_single at 1,000 μM B were 0.42 and 0.49, respectively.

Finally, we examined the effect of the combination of uORF3 and 4 (uORF3+4). The mean value of uORF3+4 under 1,000 μM B was 0.34, indicating that uORF3 and uORF4 together did not show a strong additive effect. However, the mean value of 0.34 was higher than those of UTR^{WT} and uORF2+3+4. From these results, uORF3 and 4 appeared to be indispensable factors in B-dependent downregulation, which was enhanced by the co-existence of uORF2.

1.2.5 B-Dependent Translation Mediated by the *BOR1* 5´-UTR Is Recapitulated *in Vitro*

To obtain further insights into the regulatory mechanism, it was examined whether B-dependent translation mediated by the *BOR1* 5´-UTR was reproducible *in vitro*. RNA carrying a *BOR1 5´-UTR:FLuc-*A_{30} sequence was synthesized via *in vitro* transcription and subjected to the wheat germ extract (WGE)-based *in vitro* translation system in the presence of additional boric acid. Relative

reporter activity was determined by co-translating control RNA carrying RLuc sequences. The relative reporter activity from the synthetic RNA carrying the native *BOR1* 5´-UTR (UTR^{WT}) demonstrated a dose-dependent reduction in reporter activity in the presence of 10–1,000 μM B (Fig. 5). Conversely, in a truncated-type *BOR1* 5´-UTR ($UTR^{356-251}$) containing no uORFs, no dose-dependent reduction in reporter activity was detected. This showed that the *BOR1* 5´-UTR controlled B-dependent translation in a cell-free translation system. Furthermore, disruption of all uORFs (No_uORF) markedly weakened B-dependent translational suppression since the reporter activity was decreased only in the presence of at least 500 μM B, and the extent of suppression at 1,000 μM was only 20%, while a 50% reduction was observed in the UTR^{WT} (Fig. 5). These results provide evidence that the uORF-mediated regulation is, at least in part, reproducible in a cell-free translation system.

1.2.6 Translational Reinitiation Is Involved in B-Dependent Translation

Since B-dependent translational suppression by the *BOR1* 5´-UTR was mediated mainly by uORFs 2, 3, and 4 *in planta* (Fig. 4), the mechanism of the downregulation by uORFs 2, 3, and 4 was further examined. Analysis of uORF2+3+4 confirmed its ability to induce B-dependent translational suppression *in vitro* (Fig. 5). Three possible mechanisms to reduce the translation of the main ORF (i.e., *BOR1* ORF) under high B concentrations were hypothesized: (1) ribosomes stall during the translation of uORF2, 3, and 4 under high B conditions; (2) the translation efficiency of uORF2, 3, and 4 is elevated under high B conditions; or (3) the reinitiation efficiency of translation after translating uORF2, 3, and 4 is decreased under high B concentrations.

First, the potential for ribosome stalling during uORF translation was assessed using a primer extension inhibition (toeprinting) assay. After translation of *in vitro*-transcribed RNAs uORF2+3+4 and No_uORF *in vitro*, the ribosome-associated RNAs were subjected to reverse-transcription with ^{32}P-labeled primer. The resulting cDNA products were separated in sequencing gels. Among the bands specific to uORF2+3+4 (lanes 1 and 2 compared with lanes 5 and 6 in Fig. 6A), no B-dependent increase in signal intensity was observed, suggesting that B-dependent ribosome stalling was unlikely to be a basal mechanism.

Next, the translation efficiency of uORF2, 3, and 4 under different B concentrations was investigated. Addition of hygromycin B, which inhibits translation elongation, to the *in vitro* translation system enabled the detection of the translation initiation site. In the presence of hygromycin B, doublet bands appeared 12–15 nt downstream of each uORF start codon (Fig. 6A, lanes 3 and 4), while no bands or only obscure bands were observed at the corresponding positions without hygromycin B (Fig. 6A, lanes 1 and 2), as well as in the RNA without uORFs (Fig. 6A, lanes 5–8). The intensities of the doublet bands were not appreciably changed by the addition of B. The detection of doublet bands in these positions indicated that ribosomes had been arrested at the start codons by hygromycin B, providing evidence of the translation of these uORFs. Translation of uORFs 2, 3, and 4 was further confirmed in transient expression experiments using cultured cells. *NLuc* reporter without its own start codon was translationally fused to uORF2, uORF3, uORF4, or uORF3+4 and the reporter activity was detected (Fig. 6B). The reporter gene expression indicated that the start codons of uORFs 2, 3, and 4 were functional in terms of translation initiation. The reporter activities in uORF3 fusion, uORF4 fusion and uORF3+4 fusion were much lower than uORF2 fusion, probably because uORF3 and/or uORF4 were translated only by the ribosomes that did not translate the uORF2 in these constructs. The reporter activity was not changed by B concentration, although the uORF2-fused reporter decreased under high B concentrations to 79% at 750 μM. The *in vitro* and *in vivo* analyses confirmed that uORF2, 3, and 4 were translated, and the translational efficiency was not increased under high B conditions. Therefore, mechanism (2) is unlikely.

Finally, the possible involvement of translational reinitiation was examined. In a general model of eukaryotic translation, ribosomes dissociate from mRNA after translation of an ORF. In some cases, the small subunit of ribosome resumes scanning and subsequently initiates translation of a downstream ORF after re-acquisition of translation initiation factors and the recruitment of a large subunit of ribosome. This is called translational reinitiation. Here, it was hypothesized that B concentrations would change the efficiency of translational reinitiation after the translation of uORF3 or uORF4, since uORF3 and uORF4 are basal factors for B-dependent translation *in planta* (Fig. 4). By truncation of the sequence downstream of uORF3 and 4 (uORF2+3+4_del) or expansion of the uORF length (uORF2+3+4_long),

the distance between the uORFs and the main ORF was shortened to inhibit translational reinitiation. In such constructs, the small ribosome is not expected to have sufficient time to prepare for the next translation after translation of uORF3 and 4, and thus fails to reinitiate translation at the start codon of the main ORF (Kozak, 1987; Roy et al., 2010). The reporter activities of uORF2+3+4_del and uORF2+3+4_long did not change significantly under different B concentrations (Fig. 6C), suggesting the involvement of reinitiation in B-dependent translation. In these constructs, the reporter activity was relatively lower than that of uORF2+3+4. These results suggested that reinitiation after translation of uORF3 and 4 supported a basal translation level of the main ORF under low B concentrations and that the reinitiation efficiency was reduced under high B concentrations.

1.3 Discussion

1.3.1 Conservation of Multiple uORFs Among BOR1 Orthologs

This study demonstrated that *BOR1* 5′-UTR was sufficient for the B-dependent translational suppression of the main *BOR1* ORF (Figs. 3, 4). Furthermore, the loss of B-dependency by the removal of the four uORFs, including uORF1 (AUGUAA), suggested that these uORFs are essential *cis*-elements for the B-dependent translational suppression (Figs. 3, 4). In *NIP5;1*, the AUGUAA sequence is required for B-dependent ribosome stalling, and the upstream AU-rich sequence enhances mRNA degradation (Tanaka et al., 2016). The fact that *BOR1* mRNA levels did not change was consistent with the fact that the *BOR1* 5′-UTR does not carry AU-rich sequences. In the *BOR1* 5′-UTR, uORF1 (AUGUAA) induced B-dependent suppression in cultured *A. thaliana* cells and to a lesser extent *in planta* (Figs. 3, 4). However, even in the absence of uORF1, B-dependent expression was observed in both systems and was fully observed *in planta*. These results suggest that uORF1 is not a major element required for *BOR1* translational regulation, and that this process is mainly controlled by the other uORFs, which differs from the mechanism of *NIP5;1*.

To assess the conservation of uORFs among *BOR1* homologs, the 5′-UTRs of *BOR1* homologs in vascular plants were characterized using experimentally obtained full-length cDNAs (Fig. 7). *BOR* genes were divided into two clades based on their amino acid sequences (Wakuta et al., 2015): clade I as *AtBOR1*-type for efficient B transport under B-limited conditions and clade II as *AtBOR4*-type to confer high B tolerance. The functions of several of the listed genes in B homeostasis have already been characterized, and the results support the validity of this classification (Nakagawa et al., 2007; Reid, 2007; Sutton et al., 2007; Miwa et al., 2013; Chatterjee et al., 2014). Orthologs of *AtBOR1* in clade I in vascular plants contain multiple uORFs in the 5′-UTR. Conversely, the genes belonging to clade II contain no uORFs in the 5′-UTR (Fig. 7B). These observations establish a clear link between the presence of uORFs and B transporter function, supporting the hypothesis that uORFs have a key role in downregulating the expression of *AtBOR1*-type *BOR*s under high B concentrations.

Although multiple uORFs have been commonly found in *BOR1* orthologs, the peptide sequences encoded by the uORFs do not seem to be conserved. The known models of effector molecule-

dependent translational regulation by uORFs in plants are highly dependent on conserved peptide sequences, for example in the translational regulation of *AtAdoMetDC1* by polyamine and *bZIP11* by sucrose (Hanfrey et al., 2005; Rahmani et al., 2009; Uchiyama-Kadokura et al., 2014; Yamashita et al., 2017). In this regard, it seems unlikely that *BOR1* translation is regulated in a uORF peptide-dependent manner.

Regarding BOR1 degradation, the acidic di-leucine motif and lysine residue required for selective protein degradation were found in proteins in clade I (Fig. 7B), consistent with the results of Wakuta et al. (2015). This further supports the possibility that these genes undergo two regulation steps, uORF-mediated translational suppression and protein degradation, and this two-step regulation appears to be conserved in a wide range of plant species.

1.3.2 Possible Mechanisms of *BOR1* Translational Regulation

The B-dependent translation by the *BOR1 5′*-UTR was reproduced *in vitro* (Fig. 5), suggesting that the response does not require the cell membrane or cell wall. It also suggests that boric acid or borate acts as an effector molecule that directly controls the event and this translational regulation is caused in response to local B conditions in plant cells but not systemic response.

The analysis shown in Figure 6 suggests the possibility that the B-dependent translation of the main *BOR1* ORF is controlled by the efficiency of translation reinitiation. The reinitiation efficiency can be changed by the cellular concentration of ternary complex (TC), a complex composed of Met-tRNA^{iMet} and GTP-bound eukaryotic initiation factor 2 (eIF2). Ribosomes can initiate translation only after acquisition of TCs. As studied in *GCN4* in yeast (Hinnebusch, 2005), after the translation of a uORF, high TC concentrations in cells allow ribosomes to reacquire TC rapidly so that the ribosome can translate the downstream ORF. However, when TC concentrations are low, most ribosomes cannot rebind to TC before reaching the start codon of the downstream ORF, causing them to bypass the ORF (Dever et al., 1992). A study in yeast suggested that toxic levels of boric acid inhibited TC formation via the phosphorylation of the α-subunit of eIF2 (Uluisik et al., 2011). In *A. thaliana BOR1*, it was hypothesized that the reinitiation efficiency after the translation of uORF3 and 4 decreases due to low TC levels under high B conditions, suppressing the translation of the main ORF.

As shown in Figure 3A, *BOR1* uORF3 and uORF4 carry one or both of the two important nucleotides of the Kozak sequence. It is likely that the Kozak sequence ensures a high frequency of translation initiation of these uORFs. After translation of uORF3 or uORF4, the characteristics of the *BOR1* 5′-UTR structure may enhance reinitiation. In general, the reinitiation efficiency after the translation of a uORF is affected by several *cis*-determinants, including the nucleotide sequence surrounding the uORF, the distance between the uORF and the downstream ORF (where longer distances are better), and the time required for translation of the uORF which is determined by the length of the uORF (where shorter lengths are better) and the translational elongation rate (Kozak, 1987; Gunisova et al., 2016; Hinnebusch et al., 2016). In the case of *BOR1*, the requirement of the appropriate distance between the uORF and the downstream ORF for B-dependent expression was demonstrated by the results shown in Figure 6C. Because of the frequent translation of uORF3 and uORF4 and the subsequent reinitiation ensured by the characteristics of the *BOR1* 5′-UTR structure, changes in the reinitiation efficiency after translation of uORF3 or uORF4 likely result in the B-dependent translation of the main ORF. Although it remains unclear how *BOR1* uORF2 enhances B-dependent translational suppression, the multiple uORFs in the *BOR1* 5′-UTR seem to be coordinated for the regulation of the main ORF translation.

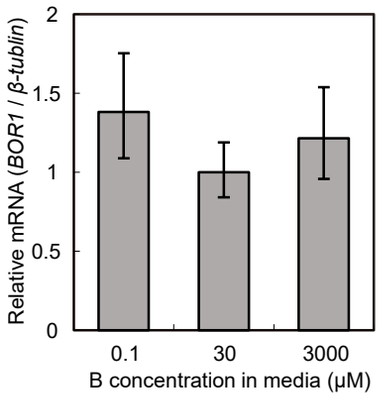

(Dr. K. Miwa)

Figure 1. *BOR1* mRNA accumulation under different B conditions.
BOR1 mRNA accumulation in Col-0 roots was determined under different B conditions. Eight-day-old Col-0 plants grown under 30 μM boric acid were transferred and incubated under 0.1, 30, or 3,000 μM boric acid for 3 d. Means ± SD are shown (n = 3).

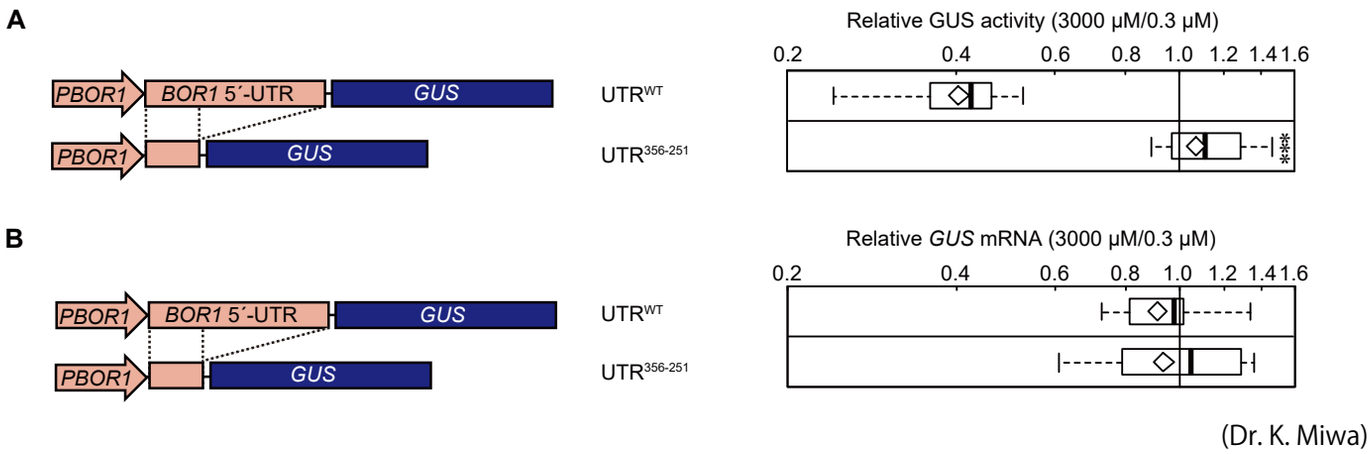

(Dr. K. Miwa)

Figure 2. Effects of *BOR1* 5′-UTR on the expression of the *BOR1* ORF. A and B, Relative GUS activity (A) and *GUS* mRNA (B) in roots of transgenic plants under toxic B conditions compared to those under low B conditions. Schematic representations of the DNA constructs used for plant transformation are shown (left). Eight- or nine-day-old plants were transferred and incubated under 0.3 or 3,000 μM boric acid for 3 d. The values are those relative to the values at 0.3 μM boric acid, which was defined as 1 in each transgenic line. Means and medians were calculated with log-transformed values. Boxplots show the distribution among six and four independent lines for UTR^{WT} and $UTR^{356-251}$, respectively. Open diamonds indicate mean values. Asterisks indicate a significant difference compared to that resulting from wild-type 5′-UTR (*** $p < 0.001$, Student' s *t*-test).

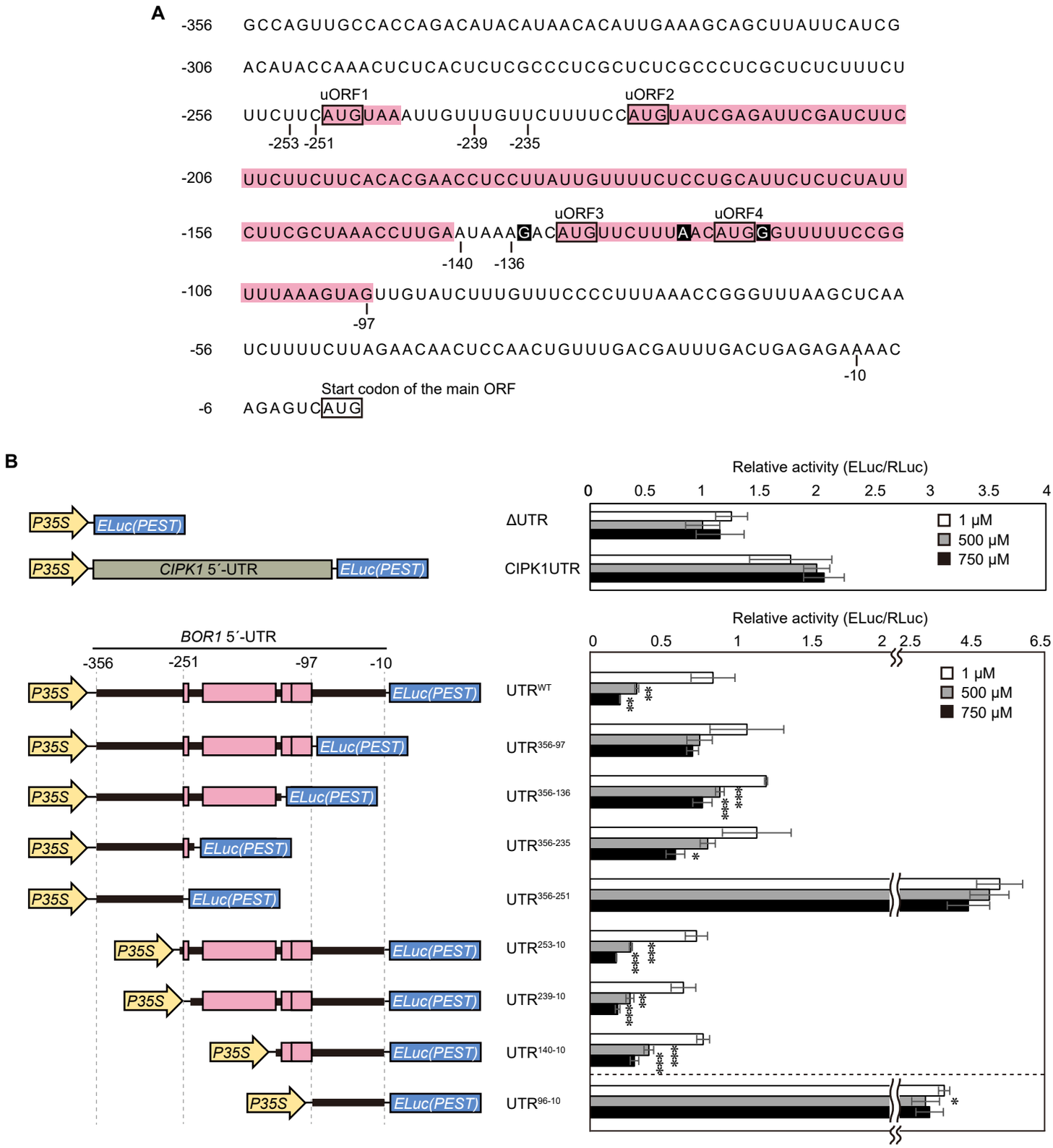

Figure 3. Effects of *BOR1* 5′-UTR nucleotide deletions on B-dependent gene expression in Arabidopsis culture cells. A, Nucleotide sequence of the *BOR1* 5′-UTR. Sequences shaded in pink represent uORFs. Nucleotides that match the Kozak sequence are highlighted in black. Start codons of uORFs and the main ORF are indicated with boxes. B, Transient expression analysis in Arabidopsis culture cells. Schematic representations of the test DNA constructs (left), and relative reporter activities (right) are shown. *CIPK1* 5′-UTR is indicated with a gray box. Bold lines and pink boxes represent the *BOR1* 5′-UTR and uORFs, respectively. Lower panel represents a *BOR1* 5′-UTR deletion series. The test and control plasmids were co-transfected into MM2d cells by electroporation. Cells were incubated in liquid media containing 1, 500, or 750 μM boric acid and reporter activities were measured by dual luciferase assay. Means ± SD of 3 independent electroporation samples are shown. The graph area is separated to two parts on different scales. Data of $UTR^{96\text{-}10}$ was obtained in an independent experiment. Asterisks indicate significant differences compared to values at 1 μM in each construct (* $p < 0.05$, ** $p < 0.01$, *** $p < 0.001$, Student' s *t*-test).

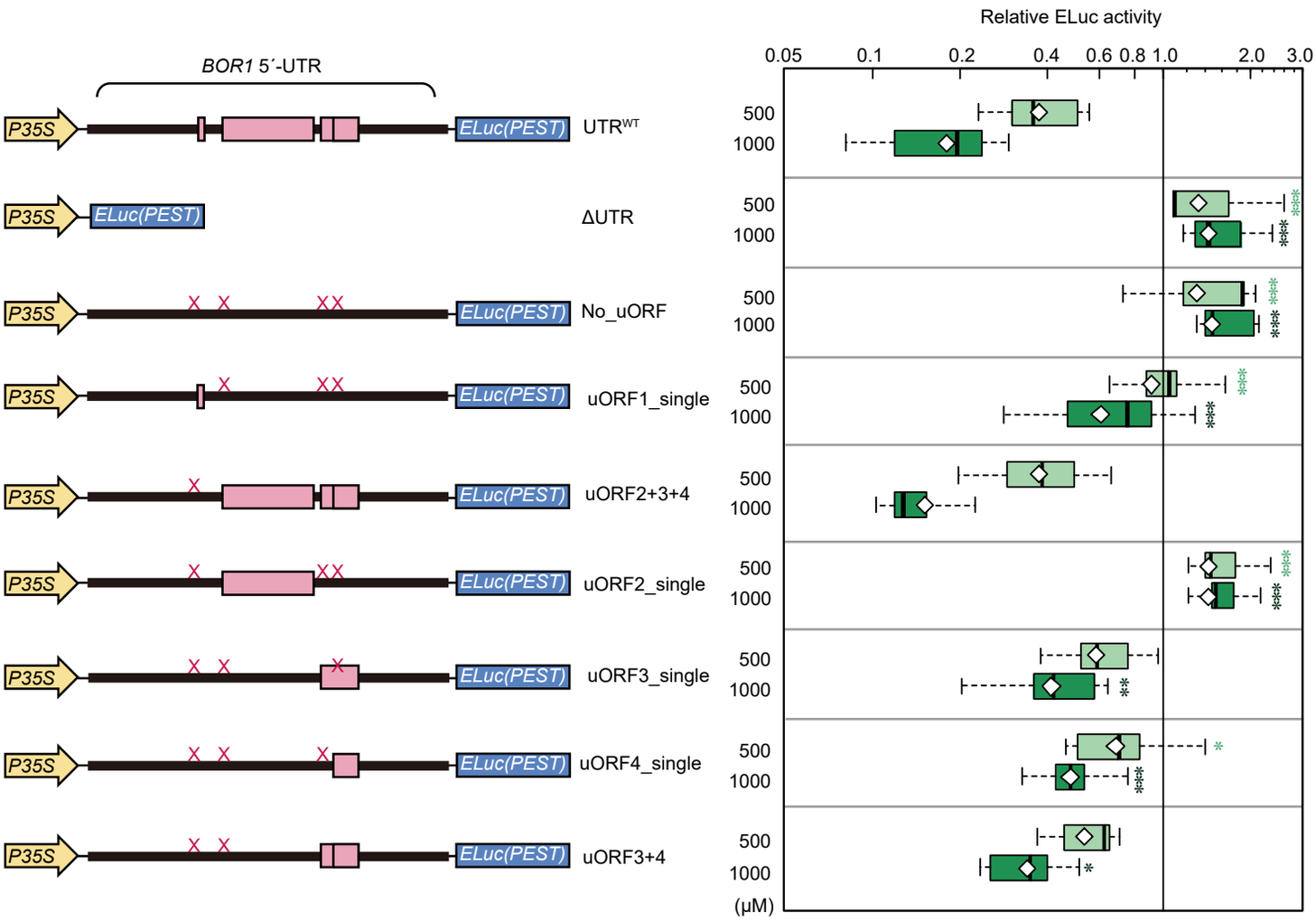

Figure 4. Effects of uORF disruptions on B-dependent gene expression driven by the *BOR1* 5′-UTR in planta. Schematic representations of the DNA constructs used for plant transformation are shown (left). Bold lines and pink boxes in the left panel represent the *BOR1* 5′-UTR and uORFs, respectively. The X marks in the 5′-UTR represent point mutations (AUG to AAG) in the start codons of uORFs. Relative reporter activities in roots under 500 and 1,000 μM boric acid are shown on the right. The transgenic plants were grown under 0.3, 500, or 1,000 μM boric acid for 12 d. Roots from 18–20 plants from one independent line were harvested as one sample. Reporter activities at 500 and 1,000 μM boric acid are shown relative to that at 0.3 μM boric acid, which was set to 1. Means and medians were calculated with log-transformed values. Boxplots show reporter activities among multiple independent transgenic lines, with that resulting from 500 μM and 1,000 μM in light and dark green, respectively. Open diamonds indicate mean values. Asterisks indicate significant differences compared to that resulting from UTR^{WT} under the same B treatment (* $p < 0.05$, ** $p < 0.01$, *** $p < 0.001$, Dunnett' s multiple comparison test). The number of tested transgenic line were as follows: UTR^{WT}, 6 lines; ΔUTR, 3 lines; No_uORF, 5 lines; uORF1_single, 7 lines; uORF2+3+4, 4 lines; uORF2_single, 5 lines; uORF3_single, 6 lines; uORF4_single, 5 lines; uORF3+4, 6 lines.

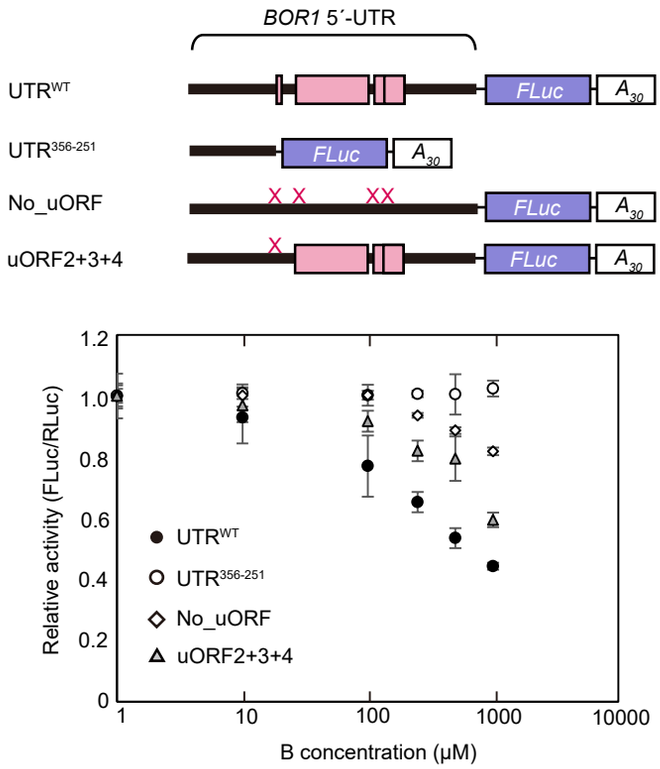

Figure 5. Translation mediated by *BOR1* 5′-UTR under different B concentrations in vitro. Synthesized test RNA and control RNA were subjected to WGE-based translation system in the presence of additional 1, 10, 100, 250, 500, and 1,000 μM boric acid. After 120 min, reporter activities were measured by dual-luciferase assay. The upper panel shows schematic representation of the synthetic test RNAs. Bold lines and pink boxes represent the *BOR1* 5′-UTR and uORFs, respectively. The X marks in the 5′-UTR represent point mutations (AUG to AAG) in the start codons of uORFs. The lower panel shows reporter activities, which are relative to reporter activity values measured at 1 μM boric acid. Means ± SD are shown (n = 3).

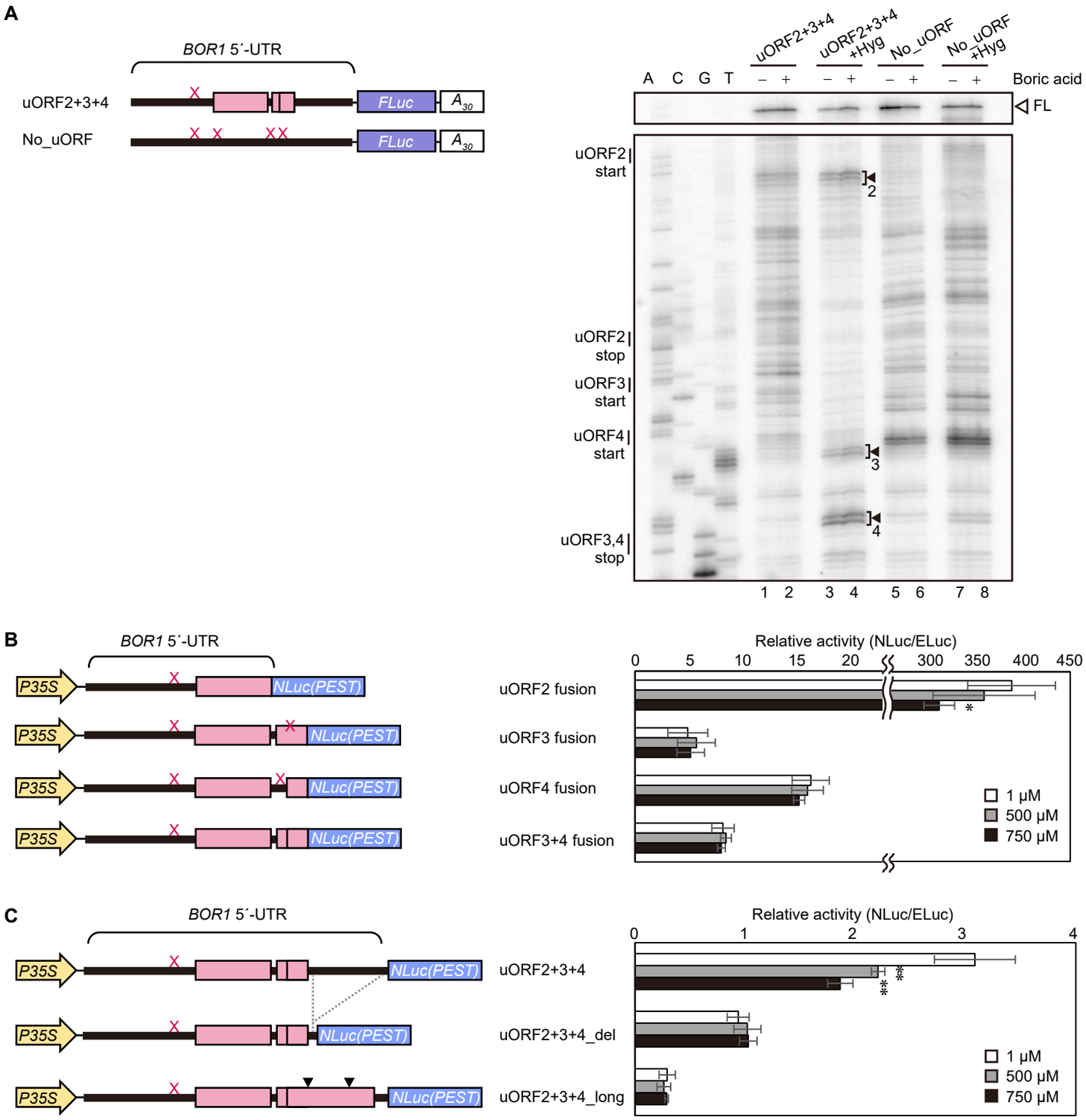

Figure 6. Examination of possible mechanisms of uORF-mediated translational regulation. A, Toeprint analysis. Synthetic RNAs were translated for 30 min in the presence (+) or absence (-) of additional boric acid (1,000 µM). +Hyg indicates that hygromycin B was added at 0 min of translation. Schematic representations of synthetic test RNAs are shown (left). Bold lines and gray boxes represent the *BOR1* 5′-UTR and uORFs, respectively. The X marks in the 5′-UTR represent point mutations (AUG to AAG) in the start codons of uORFs. The right panel shows the image of nucleotide markers and toeprint signals. Full-length primer extension products (FL) are indicated with an open arrowhead. The numbered filled arrowheads (2–4) represent Hyg-dependent toeprint signals derived from uORF2, uORF3, and uORF4, respectively. B, Reporter expression in Arabidopsis cell cultures driven by *BOR1* 5′-UTR uORFs. Schematic models of the DNA constructs used for transformation (left) and relative reporter activities (right) are shown. Reporter gene NLuc(PEST) was directly fused to uORFs. C, Reporter expression in Arabidopsis cell cultures driven by *BOR1* 5′-UTR mutated to inhibit reinitiation. Schematic models of the DNA constructs used for transformation (left) and relative reporter activities (right) are shown. In uORF2+3+4_del, 84 nucleotides (-90 to -7) were removed from downstream region of uORF3, 4. In uORF2+3+4_long, two point mutations were introduced to prevent the formation of a stop codon, resulting in elongation of uORF3, 4. Black arrowheads indicate the positions of nucleotide substitutions. Asterisks indicate significant differences compared to reporter activity values measured at 1 µM boric acid for each construct (* $p < 0.05$, ** $p < 0.01$, Student' s *t*-test).

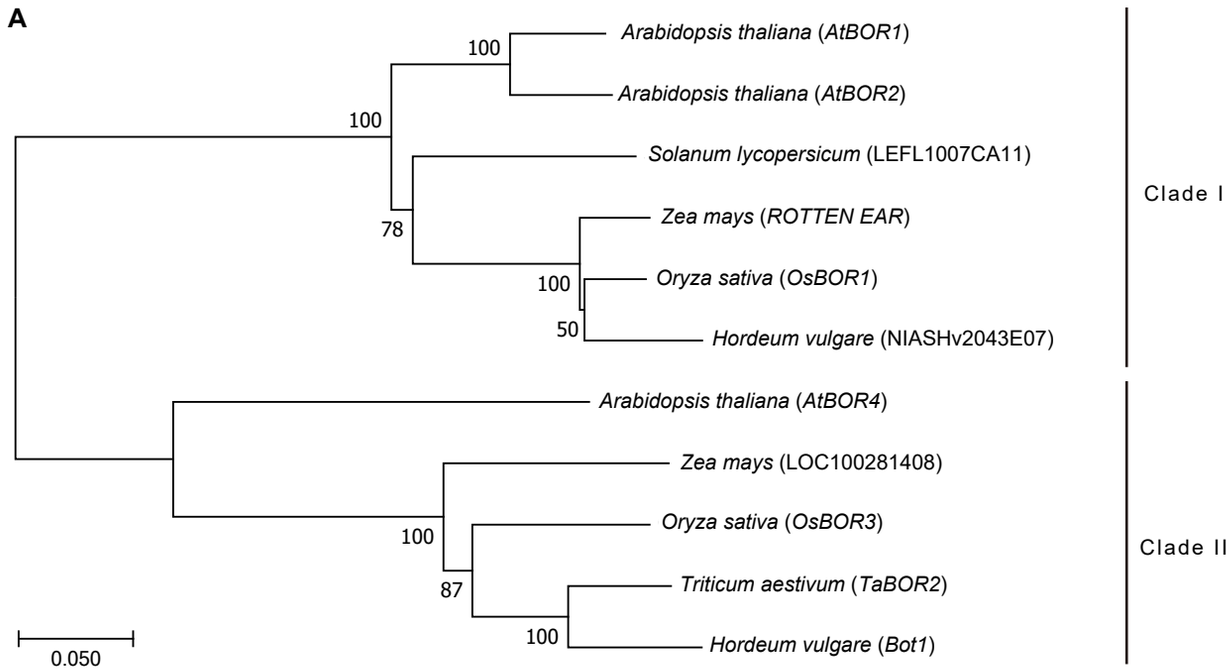

B

Plant species	Gene name, locus	Length of 5´-UTR (nt)	No. of uORFs	Tyrosine based motifs		Acidic di-leucine motif	Lysine residue
Arabidopsis thaliana	*AtBOR1*	356	4	YDNM	YHHM	EIDDLL	FKG
Arabidopsis thaliana	*AtBOR2*	415	4	YGNM	YNQM	EIDDLL	FKG
Solanum lycopersicum	LEFL1007CA11	318	2	YGNM	YQQM	EIDDLL	FKG
Zea mays	*ROTTEN EAR*	270	4	YGSM	YQQM	EIDDLL	FKG
Oryza sativa	*OsBOR1*	324	5	YGSM	YQQM	EIDDLL	FKG
Hordeum vulgare	NIASHv2043E07	381	5	YNSM	YHQI	EIDDLL	FKG
Arabidopsis thaliana	*AtBOR4*	106	0	YENM	FIEM	HLDAYL	FNP
Zea mays	LOC100281408	182	0	YGKM	FIKM	HIEAHL	FDP
Oryza sativa	*OsBOR3*	140	0	YGKM	FIEM	HIEAHL	FEP
Triticum aestivum	*TaBOR2*	141	0	YGKM	FIQM	YIEAHL	FEP
Hordeum vulgare	*Bot1*	118	0	YGKM	FIEM	HIEAHL	FEP

Figure 7. The presence of uORFs in *BOR1* homologs among vascular plants.
A, Phylogenetic tree of *BOR1* homologs. B, The presence of uORFs in 5′-UTRs and key amino acids for selective protein degradation in protein sequences.

Homologous genes of *AtBOR1* were identified by TBLASTN in the NCBI database (https://www.ncbi.nlm.nih.gov/). The experimentally obtained cDNA records which contain 5′-UTR sequences were screened. One representative gene was selected for each clade from one plant species under the following rules: Among the multiple genes in the same clade, and cDNA records derived from the same gene locus in different cultivars, cDNAs used in the published functional characterization were selected. For Arabidopsis, three out of seven *BOR* family members are shown, whose functions were experimentally characterized. cDNA sequences were obtained from GenBank as following accession numbers; *AtBOR1*, BT000732; *AtBOR2*, AY074323; LEFL1007CA11, AK320292.1; *ROTTEN EAR*, KP751214.1; *OsBOR1*, AK070617.1; NIASHv2043E07, AK366461.1; *AtBOR4*, AK317661 for 5′-UTR sequence and AY069887 for protein sequence; LOC100281408, EU956610.1; *OsBOR3*, AK072421.1; *TaBOR2*, EU220225.1; *Bot1*, EF660435.1.

The amino acid sequences of BOR1 homologous proteins were aligned by MUSCLE with default parameters. The phylogenetic relationships were inferred using the Neighbor-Joining method (Saitou and Nei, 1987). The bootstrap values (1000 replicates) are shown next to the branches (Felsenstein, 1985) in (A). The evolutionary distances were computed using the Poisson correction method (Zuckerkandl and Pauling, 1965) and are in the units of the number of amino acid substitutions per site. There were a total of 653 positions in the final dataset. Phylogenetic analyses were conducted in MEGA7 (Kumar et al., 2016).

Table 1. Plasmids and primers used for DNA construction.

Plasmid ID	Plasmid Used name	Reporter	Backbone	Primer set (Forward-Reverse)
GUS mRNA level & protein activity assay				
pTF462	UTR^{WT}	GUS	pBIN19	-
pTF463	$UTR^{356-251}$	GUS	pBIN19	-
Transient assay of deletion series in cultured cells				
pIA1	ΔUTR	ELuc(PEST)	pUC19	80-81
pIA13	CIPK1UTR	ELuc(PEST)	pUC19	200-201
pIA2	UTR^{WT}	ELuc(PEST)	pUC19	1794-83
pIA6	UTR^{356-97}	ELuc(PEST)	pUC19	1794-87
pIA19	$UTR^{356-136}$	ELuc(PEST)	pUC19	1794-208
pIA20	$UTR^{356-235}$	ELuc(PEST)	pUC19	1794-209
pIA22	$UTR^{356-251}$	ELuc(PEST)	pUC19	1794-214
pIA11	UTR^{253-10}	ELuc(PEST)	pUC19	196-83
pIA17	UTR^{239-10}	ELuc(PEST)	pUC19	204-83
pIA18	UTR^{140-10}	ELuc(PEST)	pUC19	205-83
pIA71	UTR^{96-10}	ELuc(PEST)	pUC19	688-83
Point-mutation series				
pIA35	UTR^{WT}	ELuc(PEST)	pMDC99	-
pIA34	ΔUTR	ELuc(PEST)	pMDC99	-
pIA57	No_uORF	ELuc(PEST)	pMDC99	1794-83
pIA53	uORF1_single	ELuc(PEST)	pMDC99	1794-83
pIA52	uORF2+3+4	ELuc(PEST)	pMDC99	1794-83
pIA54	uORF2_single	ELuc(PEST)	pMDC99	1794-83
pIA55	uORF3_single	ELuc(PEST)	pMDC99	1794-83
pIA56	uORF4_single	ELuc(PEST)	pMDC99	1794-83
pIA58	uORF3+4	ELuc(PEST)	pMDC99	1794-83
In vitro translation & toeprint				
pIA24	UTR^{WT}	FLuc	pUC19	-
pIA28	$UTR^{356-251}$	FLuc	pUC19	-
pIA50	No uORF	FLuc	pUC19	1794-27, 28-317, 318-83 for the first PCR 1794-83 for the second PCR
pIA36	uORF2+3+4	FLuc	pUC19	1794-27, 28-83 for the first PCR 1794-83 for the second PCR
Luciferase fusion assay				
pIA65	uORF2 fusion	fused Nluc(PEST)	pUC19	450-466
pIA62	uORF3 fusion	fused Nluc(PEST)	pUC19	450-457
pIA63	uORF4 fusion	fused Nluc(PEST)	pUC19	450-457
pIA64	uORF3+4 fusion	fused Nluc(PEST)	pUC19	450-457
Reinitiation test				
pIA59	uORF2+3+4	NLuc(PEST)	pUC19	450-451
pIA60	uORF2+3+4_del	NLuc(PEST)	pUC19	450-452
pIA61	uORF2+3+4_long	NLuc(PEST)	pUC19	450-453, 454-455, 456-451 for the first PCR 450-451 for the second PCR

Table 2. Primers used in this study.

Primer No.	Name	Sequence(5´-3´)
A1	GUS Bam Nco	AGAGGATCCAACCATGGTAATGTTACGTCCTGTAGAAACCCCAAC
A2	GUS STOP Not Sac	ACAATGAATCAACAACTCTCCTGGCGGCGCGAGCTCATAGG
A3	BOR1promoter F	CATCGGATCCGTCTTAAAATACAACACCAAAAC
A4	BOR1 5UTR firstAUG R	GAATCCATGGATAAAGAAAGAGAGCGAGGGCGA
A5	BOR1 mainAUG R	AAGCCATGGCTCTGTTTTCTCTCAGTCAAATC
A6	NlucpF2	CCTTCTAGAAAGATGGCGTCGACGGTCTTCACACTCGAAGATTTC
A7	NlucpR1	CAAGAGCTCTTAGACGTTGATGCGAGCT
1B	(1-B) BOR1 uORF2 AAG	TCTCGATACTTGGAAAAGAACA
1C	(1-C) BOR1 uORF2 AAG	TCTTTTCCAAGTATCGAGATTC
2B	(2-B) BOR1 uORF3 AAG	TTAAAGAACTTGTCTTTATTCA
2C	(2-C) BOR1 uORF3 AAG	ATAAAGACAAGTTCTTTAACAT
3B	(3-B) BOR1 uORF4 AAG	GAAAAACCCTTGTTAAAGAACA
3C	(3-C) BOR1 uORF4 AAG	TCTTTAACAAGGGTTTTTCCGG
4B	(4-B) BOR1 uORF34 AAG	CTTGTTAAAGAACTTGTCTTTATTCA
4C	(4-C) BOR1 uORF34 AAG	AAGTTCTTTAACAAGGGTTTTTCCGG
1	At2g47160Pro -1051 Forward	ATTAATAGAAAAATGTATTCTC
2	At2g47160Pro 1stATG KpnI Rev	GGGGTACCGAAGAAAGAAAGAGAGCGAG
27	BOR1 uORF1 AAG Rev	ACAATTTACTTGAAGAAAGAAA
28	BOR1 uORF1 AAG For	CTTTCTTCAAGTAAATTGTTTG
80	LUC-PEST Forward XbaI-KpnI	GCTCTAGACGGTACCGCCATGGAGAGAGAGAAGAAC
81	LUC-PEST Reverse SacI	ACGCGAGCTCAAGAATGGCATCTACACATTG
83	PromoterBOR1Reverse-KpnI	GGGGTACCTTCTCTCAGTCAAATCGTCA
87	BOR1 uORF4 KpnI R	GGGGTACCCTACTTTAAACCGGA
196	BOR1.5UTR104+XbaI	GCTCTAGATTCATGTAAATTGTT
200	AT3G17510.1 5UTR+XbaI F	GCTCTAGAAGAAGAGGAAACAAAG
201	AT3G17510.1 5UTR+KpnI R	GGGGTACCCCAATCAATCTCCT
204	pIA17-F	GCTCTAGATTGTTCTTTTC
205	pIA18-F	GCTCTAGAATAAAGACAT
208	pIA19-R-2	GGGGTACCTTTATTCAAGGT
209	pIA20-R-2	GGGGTACCAACAAACAATTTAC
214	pIA22-reverse	GGGGTACCGAAGAAAGAAAG
317	BOR1 uORF2 Rev	AGGTTTAGCGAAGAATAG
318	BOR1 uORF3-4 For	TCTTCGCTAAACCTTGA
416	BOR1_5UTR_-24to-43	TCGTCAAACAGTTGGAGTTG
450	XbaI-BOR15UTR	GCTCTAGAGCCAGTTGCCACCAGACA
451	SalI-ATG-BOR1UTR_rev	GCGTCGACTCCATGACTCTGTTTTCTCTCAGTCAAATCGTCA
452	pIA60reverse	GCGTCGACTCCATGACTCTATACAACTACTTTAAACCGGA
453	pIA61_mutation1_rev	ACAACTGCTTTAAACCGGA
454	pIA61_mutation1_for	TAAAGCAGTTGTATCTTTG
455	pIA61_mutation2_rev	GAGTTGTTCTGAGAAAAGATTG
456	pIA61_mutation2_for	CTTTTCTCAGAACAACTCCA
457	uORF3or4-NLUC_fusion	GCGTCGACGCCTTTAAACCGGAAAAAC
466	uORF2-NLUCP_fusion	GCGTCGACGCAGGTTTAGCGAAGAATAG
688	pIA71_F	GCTCTAGATTGTATCTTTG
1794	BOR1 5UTR ForXbaI	GCTCTAGAGCCAGTTGCCACCAGACATA

Table 3. Plasmids carrying point-mutated *BOR1* 5′-UTR.

Plasmid name		Presense of point-mutation in start codon			
pSP64 backbone	pMDC99 backbone	uORF1	uORF2	uORF3	uORF4
pIA50	pIA57	-	-	-	-
pIA40	pIA53	+	-	-	-
pIA36	pIA52	-	+	+	+
pIA41	pIA54	-	+	-	-
pIA42	pIA55	-	-	+	-
pIA43	pIA56	-	-	-	+
pIA49	pIA58	-	-	+	+
pIA47	-	-	+	+	-
pIA48	-	-	+	-	+

Chapter2 -Physiological significance of boron-dependent posttranscriptional regulations-

B-dependent expression of *BOR1* is controlled by two distinct regulatory mechanisms, the selective protein degradation and the translational suppression characterized in this study. In this chapter, the physiological impacts of the two downregulation mechanisms of *BOR1* was investigated *in planta* by generating transgenic *A. thaliana* plants lacking the B-dependent translational suppression and/or protein degradation described by Takano et al. (2005, 2010) (Fig. 8). The physiological significance was evaluated in three points, dose-dependency of the regulations, time-dependency, and the impacts on plant growth.

2.1 Materials and methods

2.1.1 Generation of regulation-disrupted transformants

The regulation-disrupted plants were generated by using *bor1-1* as a background plant. Basic structure of the constructs is *BOR1* promoter-(*BOR1* 5′-UTR): *BOR1-GFP*. Translational suppression and protein degradation were disrupted by a truncated 5´-UTR ($UTR^{356\text{-}251}$) (Fig. 2) and by substitution of lysine-590 with alanine (K590A) in BOR1 (Kasai et al., 2011). UTR^{WT}-$BOR1^{WT}$ and UTR^{WT}_$BOR1^{K590A}$ were derived from Takano et al. (2010) and Kasai et al. (2011), respectively.

Constructs with truncated 5′-UTR ($UTR^{356\text{-}251}$) were generated by Dr. Kyoko Miwa and Mr. Tatsuya Hirai. Used primers are listed in Table 2 in chapter 1. To express *BOR1* promoter with truncated 5′-UTR ($UTR^{356\text{-}251}$) *in planta*, a Gateway (Invitrogen) destination binary vector was generated as pTH2. A portion of *BOR1* promoter and truncated 5′-UTR was amplified with primer 1 and 2 to insert *Kpn*I sites to 3′- end. The resultant fragment was digested with *Bst*BI and *Kpn*I, and was cloned into pAT100 carrying *BOR1* promoter and 5′-UTR in pMDC32 backbone (Takano et al., 2010) to carry truncate 5′-UTR, resulting in pTH2. $BOR1^{WT}$*-GFP* and $BOR1^{K509A}$*-GFP* in pENTR/D-TOPO (invitrogen) (Takano et al. 2010; Kasai et al., 2011) were cloned into pTH2 by LR reaction to obtain $UTR^{356\text{-}251}$_$BOR1^{WT}$ (pTH3) and $UTR^{356\text{-}251}$_$BOR1^{K590A}$ (pTH4), respectively. UTR^{WT} indicates the 345 bp-long *BOR1* 5′-UTR, lacking downstream 11 nt from native 5′-UTR (356 bp) due to the plasmid construction, and

$UTR^{356\text{-}251}$ indicates 106 bp-long BOR1 5′-UTR. The linker between 5′-UTR and the start codon of *BOR1* were 82 bp and 83 bp including attB1 in UTR^{WT} and $UTR^{356\text{-}251}$, respectively.

Transformation was conducted with *Agrobacterium tumefaciens* as described in 1.1.1. Transformants were selected on solid media containing 1% (w/v) sucrose, 0.15% (w/v) gellan gum and hygromycin B (20 mg L^{-1}). T3 homozygous plants were established.

2.1.2 Immunoblotting

Microsome fraction of plant roots were subjected to immunoblotting by BOR1 antibody. Procedures were slightly modified from those described in Takano et al. (2010). The transgenic lines pAT83 (UTR^{WT}-$BOR1^{WT}$, Takano et al., 2010), pTH3 ($UTR^{356\text{-}251}$_$BOR1^{WT}$), pKKF065 (UTR^{WT}_$BOR1^{K590A}$, Kasai et al., 2011), pTH4 ($UTR^{356\text{-}251}$_$BOR1^{K590A}$) were used. Homozygous plants were grown in solid media containing 0.3, 100 and 1000 μM boric acid for 12 d. Roots (100–300 mg) were harvested and homogenized in 1 mL of homogenization buffer (250 mM Tris (pH 8.5), 290 mM sucrose, and 25 mM EDTA) by beads shocker. Protease inhibitor cocktail (Complete mini; Roche) and 75 mM 2-mercaptoethanol were added to homogenization buffer before using. Cell debris were removed by centrifugation and the supernatant was ultracentrifuged for 30 min at 100,000×*g* to obtain microsome fraction. Microsome fraction was dissolved in storage buffer (50 mM potassium phosphate (pH 6.3), 1 mM magnesium sulfate and 20% (v/v) glycerol). The samples (5 μg) were mixed with 4xNuPAGE LDS sample buffer containing 10% (v/v) 2-mercaptoethanol. The samples were incubated for 3 min at 100°C and then put on ice. They were applied to NuPAGE 4–12% (w/v) Bis-Tris gel (Invitrogen) and subjected to electrophoresis in MOS buffer at 200 V constant. Precision Plus Protein Standard Dual Color (Bio-Rad) was used as size marker. After the electrophoresis, blotting to PVDF membrane was performed with wet-transfer method. For reaction with antibodies, BOR1 polyclonal antibody was used at 400-fold dilution in CanGet Signal Solution 1 (Toyobo) and HRP-conjugated anti-rabbit IgG polyclonal antibody (GE Healthcare) was used at 6,000-fold dilution in Can Get Signal Solution 2 (Toyobo). The recognition site of the BOR1 antibody is VGNSPKPASCGRSPLNQSSSN (Target 4), and the BOR1 antibody does not recognize BOR2. For signal detection, Immobilon Western Chemiluminescent HRP substrate

(Millipore) was added on the membrane. Chemiluminescence was detected by ImageQuant LAS 4000mini (GE Healthcare). The PVDF membrane was then subjected to 0.25% (w/v) Coomassie brilliant blue R250 staining.

2.1.3 Fluorescent Imaging by Confocal Microscopy

The regulation-disrupted transgenic plants were grown on solid medium containing 0.3μM boric acid for 3 to 4 d and shifted to solid medium with 0.3 or 1,000 μM boric acid. GFP fluorescence was observed after incubation for 0, 5, 7, 10 or 24 h in root tips. Confocal images were acquired with a Leica TCS-SP8 system and a HyD hybrid detector using × 20 water immersion (NA = 0.75) objective lenses (Leica Microsystems). Pinholes were adjusted to 1 airy unit. Excitation/detection wavelengths were 488 nm/495–540 nm. Analysis of images were conducted with ImageJ software.

2.1.4 Measurement of B Concentration

The regulation-disrupted transgenic plants and control plants (Col-0 and *bor1-1*) were germinated with supply of ultrapure water for 6–8 d, and then transferred to liquid medium containing various concentrations of boric acid. After incubation for 19 d, shoots were harvested and dried at 60°C. After measurement of dry weight, shoots were digested with nitric acid and hydrogen peroxide (Wako Pure Chemicals). Digested shoots were dissociated with 2% (w/v) nitric acid and subjected to inductively coupled plasma mass spectrometry (ELAN DRC-e, Perkin-Elmer).

2.1.5 Statistical Analyses

Following statistical analyses were conducted by R software: Tukey-Kramer test for dry weight and B concentration measurements in shoots (Fig. 7).

2.2 Results

2.2.1 Translational Suppression of *BOR1* Is Induced under Higher B Concentrations than Are Required to Induce BOR1 Protein Degradation

The four DNA constructs with disruptions of translational suppression and/or protein degradation (Fig. 6) were introduced into *bor1-1*, a loss-of-function mutant of *BOR1*. Multiple independent lines exhibiting similar levels of mRNA accumulation were selected for each construct for subsequent analysis.

The protein accumulation of BOR1-GFP in the roots of the transgenic plants was examined when they were continuously grown under low (–B; 0.3 μM boric acid), sufficient (+B; 100 μM), and toxic (++B; 1,000 μM) B conditions in solid medium (Fig. 8). The result of this experiment is shown in my master's thesis (2014). BOR1-GFP levels under 0.3 μM (–B) were not appreciably different in all the transgenic lines although $UTR^{356\text{-}251}$ increased basal expression levels in transient assay in cultured cells (Fig. 3B). Similar levels of luciferase protein were also observed in the transgenic plants in UTR^{WT} and No_uORF used in the experiment in Figure 4. Taken together, the effects of elimination of uORFs on basal expression level are considered to be much smaller *in planta* than in transient expression in cultured cells possibly due to lower translational efficiency of uORFs and higher efficiency of reinitiation in *BOR1* 5´-UTR *in planta*.

In the wild-type Col-0 plants, native BOR1 accumulated under 0.3 μM (–B) and was undetectable under 100 μM (+B) and 1,000 μM (++B). The accumulation pattern of $BOR1^{WT}$-GFP in the control transgenic plants UTR^{WT}_$BOR1^{WT}$ was similar to that of native BOR1. However, in the transgenic plants defective in both translational suppression and protein degradation ($UTR^{356\text{-}251}$_$BOR1^{K590A}$), $BOR1^{K590A}$-GFP protein accumulated consistently in all of the tested B conditions (Fig. 8). This clearly demonstrated that translational suppression and protein degradation were the predominant mechanisms governing the reduction of BOR1 accumulation with this construct under sufficient and toxic B conditions.

In the $UTR^{356\text{-}251}$_$BOR1^{WT}$ line lacking translational suppression but harboring selective protein degradation, $BOR1^{WT}$-GFP accumulated at 0.3 μM (–B), but decreased at 100 μM (+B) and was further reduced at 1,000 μM (++B). This result demonstrated the induction of protein degradation at 100

μM (+B), consistent with the results of Takano et al. (2010) and the dose-dependency of the effect between 100 μM (+B) and 1,000 μM (++B). The intensities of the bands at 100 μM (+B) and 1,000 μM (++B) were slightly higher than those in the control UTR^{WT}_$BOR1^{WT}$, suggestive of the minor contribution of translational suppression. In the UTR^{WT}_$BOR1^{K590A}$ line harboring only translational suppression, no difference in $BOR1^{K590A}$-GFP accumulation was detected between 0.3 μM (–B) and 100 μM (+B), but accumulation was significantly reduced at 1,000 μM (++B). This demonstrated that translational suppression was not strongly induced at 100 μM, but was substantially induced at 1,000 μM (++B), confirming that B-dependent translational suppression was induced at a higher B concentration range than was required to induce protein degradation. These observations suggested that *BOR1* expression was downregulated mainly by protein degradation under sufficient B conditions and was further decreased by both translational suppression and protein degradation at higher B concentrations.

2.2.2 Translational Suppression Causes a More Gradual Decline of BOR1 than Protein Degradation

To investigate time-dependence of the two downregulation mechanisms, BOR1-GFP was observed in the roots of the transgenic plants, transferred from 0.3 μM (–B) to 1,000 μM (++B) in solid media (Fig. 9). In the UTR^{WT}_$BOR1^{WT}$ and $UTR^{356\text{-}251}$_$BOR1^{WT}$ lines harboring selective protein degradation, GFP intensity was decreased within 5 h as previously reported in Takano et al., (2010). In the UTR^{WT}_$BOR1^{K590A}$ line harboring only translational suppression, GFP intensity was gradually reduced within 24 h. In the $UTR^{356\text{-}251}$_$BOR1^{K590A}$ line lacking both regulation mechanisms, GFP intensity was not decreased. These indicate that translational suppression results in a more gradual decline of BOR1 than selective protein degradation.

2.2.3 Two Posttranscriptional Regulation Mechanisms Contribute to High B Tolerance

The growth of regulation-disrupted plants were characterized under low (10 μM), sufficient (100 μM),

high (250 μM), or toxic (500 μM) B conditions in hydroponic cultures (Fig. 10). Since BOR1 has an important role in the translocation of B from roots to shoots, shoot growth and B accumulation in shoots were observed. The boric acid concentration for the toxic B condition (500 μM) was set lower than that for the solid medium system (1,000 μM) because the transpiration stream is facilitated in hydroponic culture enabling more B to accumulate in shoots.

Under the low B condition (10 μM), the shoot growth of *bor1-1* was less than that of Col-0, and showed a dark green color and shrinkage of rosette leaves due to the decrease in B translocation, as previously reported (Noguchi et al., 1997). Such leaf phenotypes were not observed in all transgenic plants, indicating that $BOR1^{WT}$-GFP or $BOR1^{K590A}$-GFP, driven by the promoter with a truncated 5´-UTR, was able to complement the loss-of-function mutation of *BOR1*.

When exposed to 500 μM boric acid, the plants lacking both translational regulation and BOR1 protein degradation ($UTR^{356\text{-}251}$_$BOR1^{K590A}$) exhibited severe growth defects compared to Col-0 and the other transgenic plants (Fig. 10A, B). This suggested that the downregulation of *BOR1* was required for normal growth under high B conditions. A growth reduction was not observed in plants lacking only translational suppression ($UTR^{356\text{-}251}$_$BOR1^{WT}$) compared to the control transgenic plants (UTR^{WT}_$BOR1^{WT}$). Meanwhile, the growth of plants lacking only protein degradation (UTR^{WT}_$BOR1^{K590A}$) decreased, except for line 2, but the effect was not as severe as that observed in $UTR^{356\text{-}251}$_$BOR1^{K590A}$.

Higher B concentrations in shoots were observed in the plants with defective protein degradation ($UTR^{356\text{-}251}$_$BOR1^{K590A}$ and UTR^{WT}_$BOR1^{K590A}$, except for line 2) at or above 100 μM (Fig. 10C). This suggested that the growth reduction of these lines under high B conditions was caused by higher accumulation of B in shoots due to overloading of B by BOR1, indicating that protein degradation is the major mechanism that prevents B over-accumulation.

To clarify the effects of translational suppression in the absence of protein degradation, $UTR^{356\text{-}251}$_$BOR1^{K590A}$ and UTR^{WT}_$BOR1^{K590A}$ were compared. Under 250 and 500 μM boric acid, the B concentration in shoots was higher in $UTR^{356\text{-}251}$_$BOR1^{K590A}$ than in UTR^{WT}_$BOR1^{K590A}$. Since the B concentrations in these plants did not differ significantly under the low B condition (10 μM), the

difference in B concentrations between $UTR^{356\text{-}251}$_$BOR1^{K590A}$ and UTR^{WT}_$BOR1^{K590A}$ was likely attributable to the contribution of high B-induced translational suppression. Together, these results indicate that two posttranscriptional regulatory mechanisms induced under different ranges of boric acid concentrations contribute to reducing BOR1 accumulation and preventing overloading of B under high B conditions.

2.3 Discussion

2.3.1 Biological Significance of the Two-Step Regulation of *BOR1*

This study uncovered that expression of *BOR1* is regulated at two posttranscriptional steps, in response to B concentrations. One advantage of posttranscriptional regulation is that it is more rapid than transcriptional regulation. Importance of rapid expression regulation of B transporters has been suggested by mathematical modelling simulating B transport by NIP5;1 and BOR transporters in *A. thaliana* root cells (Sotta et al., 2017). In the mathematical modelling, when the swiftness of the regulation was decreased than experimentally observed regulation, fluctuation of B flow occurred and root cells were occasionally exposed to high concentration of B. It is possible to speculate that plants control expression of *BOR1* at posttranscriptional levels because rapid regulation of B transporters is required for maintaining robust B flow inside their bodies.

It is reasonable to assume that plants possess multiple regulatory mechanisms that tightly control the expression of transporters. To date, several multi-step nutrient-dependent regulatory mechanisms in plant nutrient transporter genes have been reported. For example, for *A. thaliana PHOSPHATE TRANSPORTER 1;1* (*PHT1;1*), which encodes a phosphate transporter for phosphate uptake in roots, phosphorus deficiency increases mRNA accumulation (Muchhal et al., 1996) and enhances the exit of the protein from the endoplasmic reticulum (Gonzalez et al., 2005; Bayle et al., 2011), whereas protein degradation is induced by phosphorus repletion (Bayle et al., 2011). In the case of *A. thaliana IRON-REGULATED TRANSPORTER 1* (*IRT1*), which encodes a metal transporter, mRNA levels are upregulated under low iron conditions (Eide et al., 1996; Connolly et al., 2002), and the protein is targeted from early endosomes/*trans*-Golgi network to the plasma membrane under low concentrations of non-iron metals (Barberon et al., 2014). Notably, the two steps of posttranscriptional regulation of *BOR1* are induced at different B concentration ranges (Fig. 8). Most studies on nutrient transporters have focused on one nutrient-dependent regulatory mechanism under two nutrient conditions in each experimental system, making it difficult to directly compare differences in the concentration range required to induce the respective mechanisms. The physiological role of *BOR1* two-step regulation to directly control protein quantity can be considered as follows. Under sufficient B

conditions, the accumulation of BOR1 is regulated mostly by protein degradation; therefore, it is rapidly (Fig. 9) and precisely altered in response to changes in external B concentrations. On the other hand, under continuous toxic B concentrations, BOR1 is not required and can be harmful; therefore, the synthesis of BOR1 is stopped via translation suppression. This two-step regulation under different B concentrations is likely beneficial for the cost-effective regulation of *BOR1* expression. The presence of multiple regulatory mechanisms induced under different nutrient concentrations suggests that plants use independent regulatory mechanisms to fulfill the demands of fine-tuning nutrient transport.

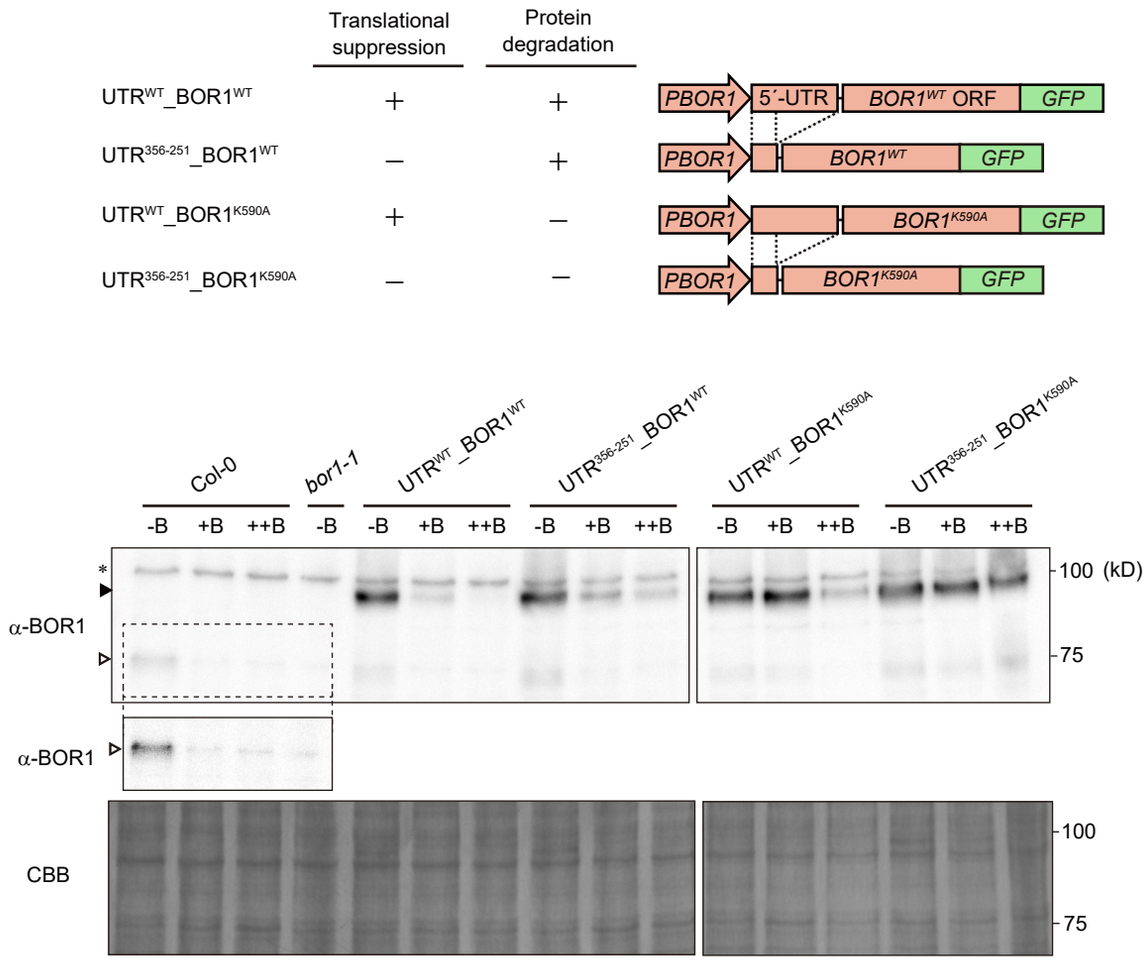

Figure 8. BOR1-GFP accumulation under different boric acid concentrations in transgenic plants with various disruptions in *BOR1* regulation mechanisms. The upper panel shows schematic representations of DNA constructs. The presence and absence of post-transcriptional regulations are indicated with + and -, respectively. GFP was fused to the C terminus of BOR1^{WT}/BOR1^{K590A}. The DNA constructs were introduced into *bor1-1*, a *BOR1* loss-of-function mutant. The lower panel shows immunoblot analysis of the microsome fraction from plant roots. Plants were grown for 12 d on solid media containing 0.3 μM (-B), 100 μM (+B), and 1,000 μM (++B) of boric acid. A representative accumulation pattern is shown. White and black arrowheads indicate positions of protein bands corresponding to native BOR1 and BOR1-GFP, respectively. The asterisk indicates non-specific bands. The protein bands that resemble that of native BOR1 in the *bor1-1* transformed lines could be degradation products of BOR1-GFP. Images of two different membranes are shown. For Col-0 and *bor1-1*, the protein bands corresponding to native BOR1 (dashed box) are shown in higher contrast in the cropped image. Membrane staining with Coomassie Brilliant Blue (CBB) is depicted below as a loading control.

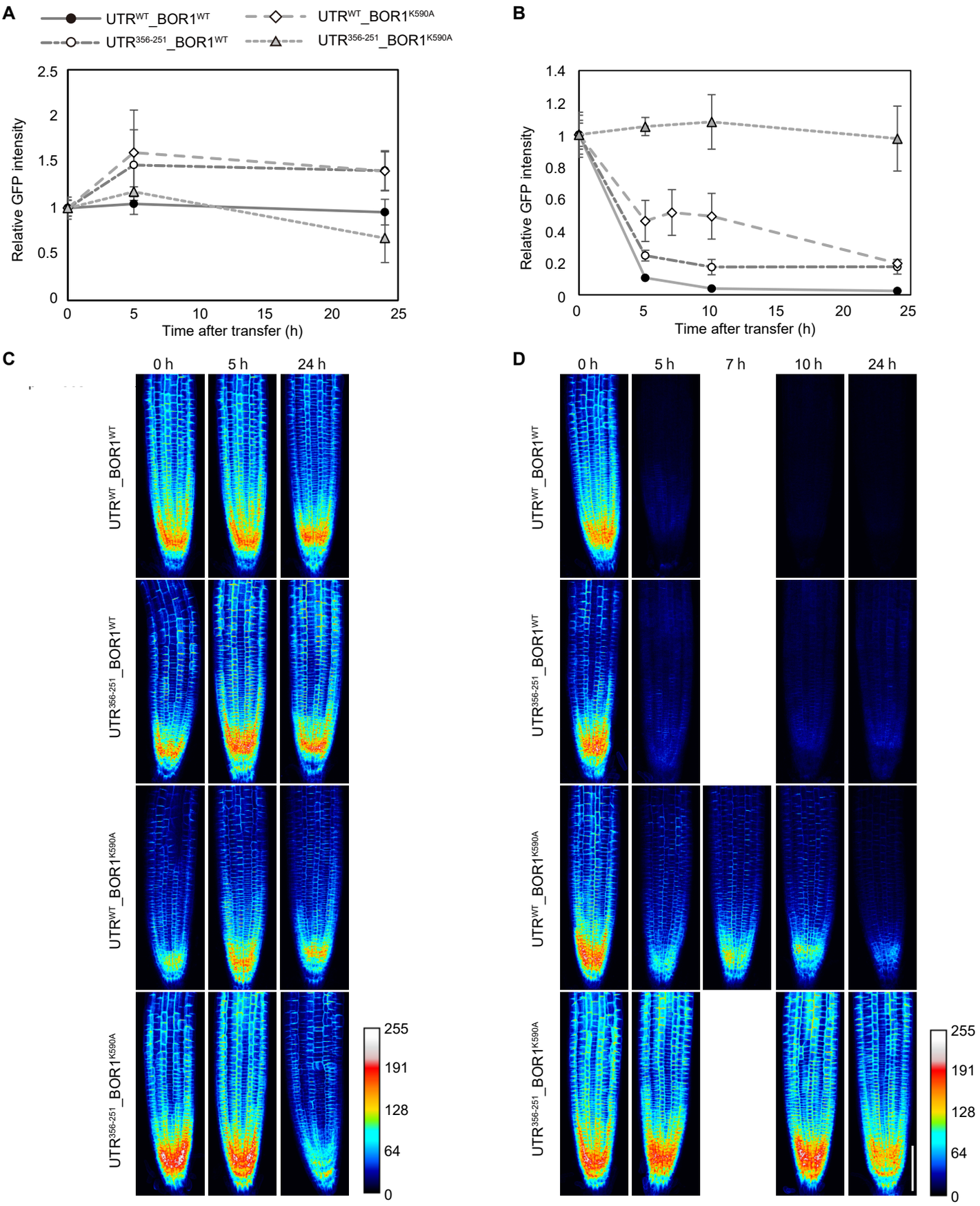

Figure 9. Time-course analysis of BOR1-GFP levels.

A to D, BOR1-GFP accumulation was quantified by fluorescent imaging at different time points in transgenic plants disrupted in *BOR1* regulation. Three- or four-day-old plants grown under 0.3 μM boric acid were transferred to 0.3 (-B) or 1,000 μM (++B) boric acid medium and incubated for 0, 5, 7, 10, or 24 h. Quantification of GFP intensity in root tips and representative images of plants treated under 0.3 (A, C) or 1,000 μM boric acid (B, D) are shown. Z-stack images of root tips were taken at 5 μm intervals for 25 slices and sum image was projected by ImageJ software. The mean GFP intensity in projected images (ROI: 150 × 450 μm) was obtained. A and B, GFP intensity at each time point as a relative value compared to that at 0 h. Means ± SD are shown (n = 3 or 4). C and D, Sum images of root tips of each time point, projected in “Royal” color code. Relative GFP intensities are shown for each transgenic line. Bar = 100 μm.

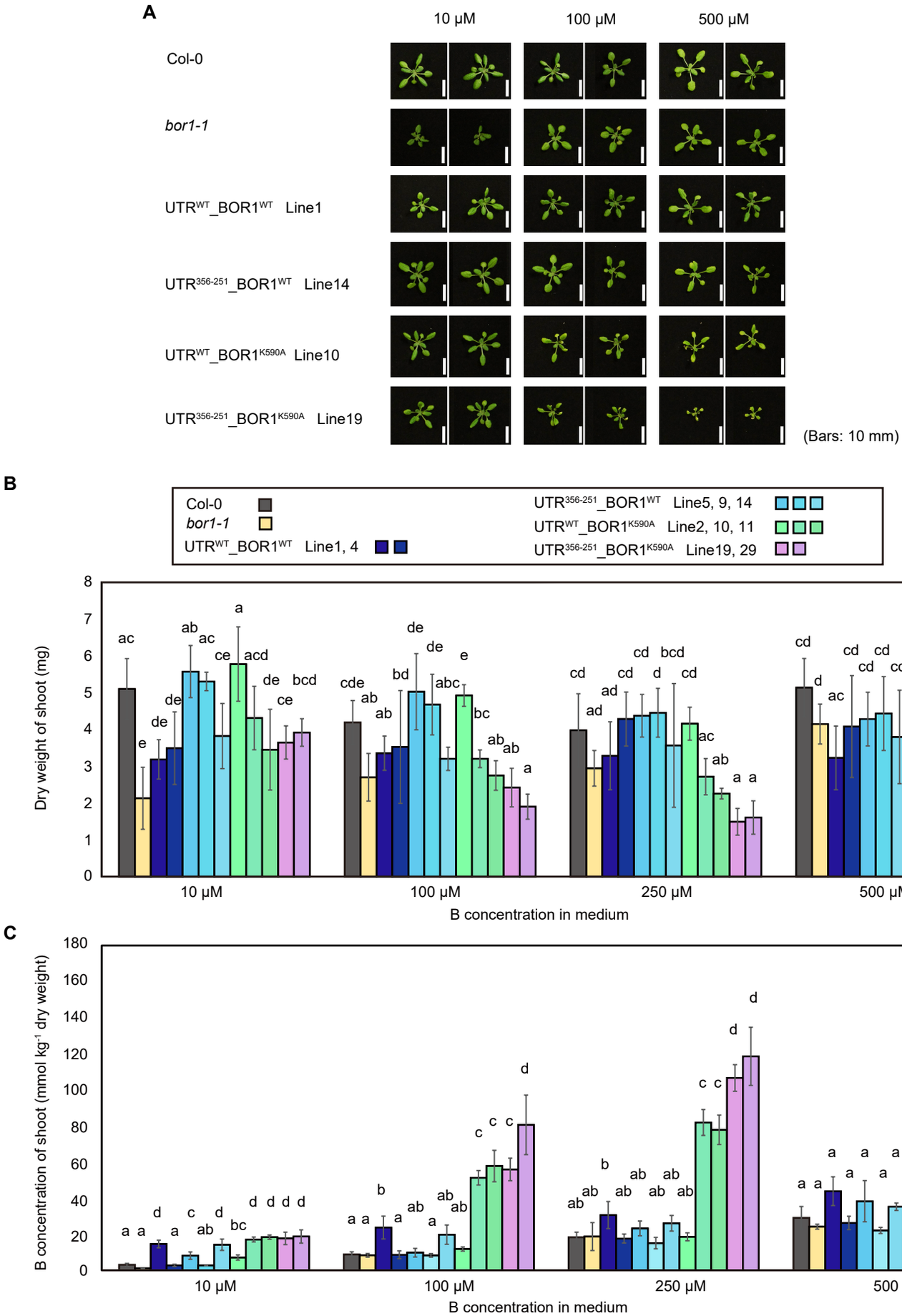

Figure 10. Growth and B concentration in hydroponic culture-grown shoots of transgenic plants with various disruptions in *BOR1* regulation mechanisms. A, Shoot growth of the transgenic plants. After germination, seedlings were transferred to liquid media containing 10, 100, 250, or 500 μM boric acid and incubated for 19 d. B and C, Shoot dry weight (B) and B concentration (C). Means ± SD are shown (n = 3–7). Different letters indicate significant differences among plants under the same B treatment ($p < 0.05$, Tukey-Kramer test).

Conclusion

This thesis revealed that *BOR1* expression is regulated by translational suppression, which, together with the selective degradation of BOR1, contributes to reducing the accumulation of BOR1 under high B conditions against B toxicity. Furthermore, it was confirmed that reduction of BOR1 by the two posttranscriptional regulatory mechanisms are induced in different dose-dependent and time-dependent manners. This study successfully depicted fine-tuning of nutrient uptake by expression regulation of a nutrient transporter in plants.

Acknowledgements

First and foremost, I would like to express my deepest gratitude to my supervisor Dr. Kyoko Miwa for guiding me throughout my student life. She had given me a lot of advice and helping hands even when I was in depression.

I would like to express my appreciation to Prof. Masaaki Morikawa for valuable discussions and continuous support. Having meetings with him and his laboratory members was always inspiring.

I would like to thank Dr. Ken-ichi Yamazaki for kind encouragement in my research life.

I am deeply grateful to Prof. Yoshifumi Yamaguchi and Dr. Takeo Sato for attending my Ph.D defense as examiners.

I would like to express my gratitude to Prof. Satoshi Naito and Dr. Hitoshi Onouchi for helpful advices and discussions, especially on analyses for translational regulation. This work would not been fulfilled without them. I am also grateful to Mr. Noriya Hayashi for supporting toeprint assay.

I would like to express my sincere appreciation to Prof. Junpei Takano and his laboratory members in Osaka Prefecture University, for giving me warm helping hands during my stay in their laboratory.

I sincerely appreciate to the members of Miwa laboratory, including members who have already graduated. Spending research time with them was fruitful.

I would like to acknowledge JSPS for financial support.

Last but not least, I sincerely thank my friends and my family for supporting me all the time.

References

Aibara I (2014) Molecular mechanisms and physiological roles of boron-dependent expression of a boron transporter BOR1 in *Arabidopsis thaliana*, Master thesis, Hokkaido University

Argust P (1998) Distribution of boron in the environment. Biol Trace Elem Res 66: 131-143

Barberon M, Dubeaux G, Kolb C, Isono E, Zelazny E, Vert G (2014) Polarization of IRON-REGULATED TRANSPORTER 1 (IRT1) to the plant-soil interface plays crucial role in metal homeostasis. Proc Natl Acad Sci USA 111: 8293-8298

Bayle V, Arrighi JF, Creff A, Nespoulous C, Vialaret J, Rossignol M, Gonzalez E, Paz-Ares J, Nussaume L (2011) *Arabidopsis thaliana* high-affinity phosphate transporters exhibit multiple levels of posttranslational regulation. Plant Cell 23: 1523-1535

Bolanos L, Lukaszewski K, Bonilla I, Blevins D (2004) Why boron? Plant Physiol Biochem 42: 907-912

Cañon P, Aquea F, Rodriguez-Hoces de la Guardia A, Arce-Johnson P (2013) Functional characterization of *Citrus macrophylla BOR1* as a boron transporter. Physiol Plant 149: 329-339

Chatterjee M, Tabi Z, Galli M, Malcomber S, Buck A, Muszynski M, Gallavotti A (2014) The boron efflux transporter ROTTEN EAR is required for maize inflorescence development and fertility. Plant Cell 26: 2962-2977

Chiba Y, Sakurai R, Yoshino M, Ominato K, Ishikawa M, Onouchi H, Naito S (2003) *S*-adenosyl-L-methionine is an effector in the posttranscriptional autoregulation of the cystathionine γ-synthase gene in *Arabidopsis*. Proc Natl Acad Sci USA 100: 10225-10230

Connolly EL, Fett JP, Guerinot ML (2002) Expression of the IRT1 metal transporter is controlled by metals at the levels of transcript and protein accumulation. Plant Cell 14: 1347-1357

Dever TE, Feng L, Wek RC, Cigan AM, Donahue TF, Hinnebusch AG (1992) Phosphorylation of initiation factor 2α by protein kinase GCN2 mediates gene-specific translational control of *GCN4* in yeast. Cell 68: 585-596

Dordas C, Chrispeels MJ, Brown PH (2000) Permeability and channel-mediated transport of boric acid across membrane vesicles isolated from squash roots. Plant Physiol 124: 1349-1362

Durbak AR, Phillips KA, Pike S, O'Neill MA, Mares J, Gallavotti A, Malcomber ST, Gassmann W, McSteen P (2014) Transport of boron by the *tassel-less1* aquaporin is critical for vegetative and reproductive development in maize. Plant Cell 26: 2978-2995

Ebina I, Takemoto-Tsutsumi M, Watanabe S, Koyama H, Endo Y, Kimata K, Igarashi T, Murakami K, Kudo R, Ohsumi A, Noh AL, Takahashi H, Naito S, Onouchi H (2015) Identification of novel *Arabidopsis thaliana* upstream open reading frames that control expression of the main coding sequences in a peptide sequence-dependent manner. Nucleic Acids Res 43: 1562-1576

Eide D, Broderius M, Fett J, Guerinot ML (1996) A novel iron-regulated metal transporter from plants identified by functional expression in yeast. Proc Natl Acad Sci USA 93: 5624-5628

Felsenstein J (1985) Confidence limits on phylogenies: An approach using the bootstrap. Evolution 39:783-791

Fujiwara T, Hirai MY, Chino M, Komeda Y, Naito S (1992) Effects of sulfur nutrition on expression of the soybean seed storage protein genes in transgenic petunia. Plant Physiol 99: 263-268

Funakawa H, Miwa K (2015) Synthesis of borate cross-linked rhamnogalacturonan II. Front Plant Sci 6: 223

Ge Z, Rubio G, Lynch JP (2000) The importance of root gravitropism for inter-root competition and phosphorus acquisition efficiency: results from a geometric simulation model. Plant Soil 218: 159-171

Gonzalez E, Solano R, Rubio V, Leyva A, Paz-Ares J (2005) PHOSPHATE TRANSPORTER TRAFFIC FACILITATOR1 is a plant-specific SEC12-related protein that enables the endoplasmic reticulum exit of a high-affinity phosphate transporter in *Arabidopsis*. Plant Cell 17: 3500-3512

Gruber BD, Giehl RF, Friedel S, von Wiren N (2013) Plasticity of the Arabidopsis root system under nutrient deficiencies. Plant Physiol 163: 161-179

Gunisova S, Beznoskova P, Mohammad MP, Vlckova V, Valasek LS (2016) In-depth analysis of cis-determinants that either promote or inhibit reinitiation on *GCN4* mRNA after translation of its four short uORFs. RNA 22: 542-558

Hanaoka H, Uraguchi S, Takano J, Tanaka M, Fujiwara T (2014) OsNIP3;1, a rice boric acid channel,

regulates boron distribution and is essential for growth under boron-deficient conditions. Plant J 78: 890-902

Hanfrey C, Elliott KA, Franceschetti M, Mayer MJ, Illingworth C, Michael AJ (2005) A dual upstream open reading frame-based autoregulatory circuit controlling polyamine-responsive translation. J Biol Chem 280: 39229-39237

Hayashi N, Sasaki S, Takahashi H, Yamashita Y, Naito S, Onouchi H (2017) Identification of *Arabidopsis thaliana* upstream open reading frames encoding peptide sequences that cause ribosomal arrest. Nucleic Acids Res. 45:8844-8858

Hellen CU, Sarnow P (2001) Internal ribosome entry sites in eukaryotic mRNA molecules. Genes Dev 15: 1593-1612

Heppell J, Talboys P, Payvandi S, Zygalakis KC, Fliege J, Withers PJ, Jones DL, Roose T (2015) How changing root system architecture can help tackle a reduction in soil phosphate (P) levels for better plant P acquisition. Plant Cell Environ 38: 118-28

Hinnebusch AG (2005) Translational regulation of *GCN4* and the general amino acid control of yeast. Annu Rev Microbiol 59: 407-450

Hinnebusch AG, Ivanov IP, Sonenberg N (2016) Translational control by 5'-untranslated regions of eukaryotic mRNAs. Science 352: 1413-1416

Jobbagy EG and Jackson RB (2001) The distribution of soil nutrients with depth: Global patterns and the imprint of plants. Biogeochemistry 53: 51-77

Joshi CP, Zhou H, Huang X, Chiang VL (1997) Context sequences of translation initiation codon in plants. Plant Mol Biol 35: 993-1001

Kasai K, Takano J, Miwa K, Toyoda A, Fujiwara T (2011) High boron-induced ubiquitination regulates vacuolar sorting of the BOR1 borate transporter in *Arabidopsis thaliana*. J Biol Chem 286: 6175-6183

Kozak M (1986) Point mutations define a sequence flanking the AUG initiator codon that modulates translation by eukaryotic ribosomes. Cell 44: 283-292

Kozak M (1987) Effects of intercistronic length on the efficiency of reinitiation by eucaryotic ribosomes.

Mol Cell Biol 7: 3438-3445

Kumar S, Stecher G, Tamura K (2016) MEGA7: Molecular Evolutionary Genetics Analysis version 7.0 for bigger datasets.Mol Biol Evol 33:1870-1874

Leaungthitikanchana S, Fujibe T, Tanaka M, Wang S, Sotta N, Takano J, Fujiwara T (2013) Differential expression of three *BOR1* genes corresponding to different genomes in response to boron conditions in hexaploid wheat (*Triticum aestivum* L.). Plant Cell Physiol 54: 1056-1063

Lopez-Bucio J, Hernandez-Abreu E, Sanchez-Calderon L, Nieto-Jacobo MF, Simpson J, Herrera-Estrella L (2002) Phosphate availability alters architecture and causes changes in hormone sensitivity in the Arabidopsis root system. Plant Physiol 129: 244-256

Marschner H (2012) Mineral Nutrition of Higher Plants, 3rd ed. (San Diego, CA: Academic Press).

Menges M, Murray JA (2002) Synchronous Arabidopsis suspension cultures for analysis of cell-cycle gene activity. Plant J 30: 203-212

Miwa K, Takano J, Omori H, Seki M, Shinozaki K, Fujiwara T (2007) Plants Tolerant of High Boron Levels. Science 318: 1417

Miwa K, Aibara I, Fujiwara T (2014) *Arabidopsis thaliana BOR4* is upregulated under high boron conditions and confers tolerance to high boron. Soil Sci Plant Nutr 60: 349-355

Miwa K, Wakuta S, Takada S, Ide K, Takano J, Naito S, Omori H, Matsunaga T, Fujiwara T (2013) Roles of BOR2, a boron exporter, in cross linking of rhamnogalacturonan II and root elongation under boron limitation in Arabidopsis. Plant Physiol 163: 1699-1709

Muchhal US, Pardo JM, Raghothama KG (1996) Phosphate transporters from the higher plant *Arabidopsis thaliana*. Proc Natl Acad Sci USA 93: 10519-10523

Nable RO, Banuelos GS, Paull JG (1997) Boron toxicity. Plant Soil 193: 181-198

Nakagawa Y, Hanaoka H, Kobayashi M, Miyoshi K, Miwa K, Fujiwara T (2007) Cell-type specificity of the expression of Os *BOR1*, a rice efflux boron transporter gene, is regulated in response to boron availability for efficient boron uptake and xylem loading. Plant Cell 19: 2624-2635

Noguchi K, Yasumori M, Imai T, Naito S, Matsunaga T, Oda H, Hayashi H, Chino M, Fujiwara T (1997) bor1-1, an *Arabidopsis thaliana* mutant that requires a high level of boron. Plant Physiol 115:

901-906

O'Neill MA, Eberhard S, Albersheim P, Darvill AG (2001) Requirement of borate cross-linking of cell wall rhamnogalacturonan II for *Arabidopsis* growth. Science 294: 846-849

O'Neill MA, Ishii T, Albersheim P, Darvill AG (2004) Rhamnogalacturonan II: structure and function of a borate cross-linked cell wall pectic polysaccharide. Annu Rev Plant Biol 55: 109-139

Park H, Schlesinger WH (2002) Global biogeochemical cycle of boron. Global Biogeochem Cycles 16: 1072

Perez-Castro R, Kasai K, Gainza-Cortes F, Ruiz-Lara S, Casaretto JA, Pena-Cortes H, Tapia J, Fujiwara T, Gonzalez E (2012) *VvBOR1*, the grapevine ortholog of *AtBOR1*, encodes an efflux boron transporter that is differentially expressed throughout reproductive development of *Vitis vinifera* L. Plant Cell Physiol 53: 485-494

Rahmani F, Hummel M, Schuurmans J, Wiese-Klinkenberg A, Smeekens S, Hanson J (2009) Sucrose control of translation mediated by an upstream open reading frame-encoded peptide. Plant Physiol 150: 1356-1367

Reid R (2007) Identification of boron transporter genes likely to be responsible for tolerance to boron toxicity in wheat and barley. Plant Cell Physiol 48: 1673-1678

Reid RJ, Hayes JE, Post A, Stangoulis JCR, Graham RD (2004) A critical analysis of the causes of boron toxicity in plants. Plant Cell Environ 27: 1405-1414

Roy B, Vaughn JN, Kim BH, Zhou F, Gilchrist MA, Von Arnim AG (2010) The h subunit of eIF3 promotes reinitiation competence during translation of mRNAs harboring upstream open reading frames. RNA 16: 748-761

Rubio G, Liao H, Yan XL, Lynch JP (2003) Topsoil foraging and its role in plant competitiveness for phosphorus in common bean. Crop Science 43: 598-607

Saitou N, Nei M (1987) The neighbor-joining method: A new method for reconstructing phylogenetic trees. Mol Biol Evol 4:406-425

Sakamoto T, Inui YT, Uraguchi S, Yoshizumi T, Matsunaga S, Mastui M, Umeda M, Fukui K, Fujiwara T (2011) Condensin II alleviates DNA damage and is essential for tolerance of boron overload

stress in *Arabidopsis*. Plant Cell 23: 3533-3546

Seki M, Narusaka M, Kamiya A, Ishida J, Satou M, Sakurai T, Nakajima M, Enju A, Akiyama K, Oono Y, Muramatsu M, Hayashizaki Y, Kawai J, Carninci P, Itoh M, Ishii Y, Arakawa T, Shibata K, Shinagawa A, Shinozaki K (2002) Functional annotation of a full-length *Arabidopsis* cDNA collection. Science 296: 141-145

Shorrocks VM (1997) The occurrence and correction of boron deficiency. Plant Soil 193: 121-148

Sotta N, Duncan S, Tanaka M, Sato T, Maree AF, Fujiwara T, Grieneisen VA (2017) Rapid transporter regulation prevents substrate flow traffic jams in boron transport. Elife 6: e27038

Sugio T, Matsuura H, Matsui T, Matsunaga M, Nosho T, Kanaya S, Shinmyo A, Kato K (2010) Effect of the sequence context of the AUG initiation codon on the rate of translation in dicotyledonous and monocotyledonous plant cells. J Biosci Bioeng 109: 170-173

Sutton T, Baumann U, Hayes J, Collins NC, Shi BJ, Schnurbusch T, Hay A, Mayo G, Pallotta M, Tester M, Langridge P (2007) Boron-toxicity tolerance in barley arising from efflux transporter amplification. Science 318: 1446-1449

Takano J, Noguchi K, Yasumori M, Kobayashi M, Gajdos Z, Miwa K, Hayashi H, Yoneyama T, Fujiwara T (2002) *Arabidopsis* boron transporter for xylem loading. Nature 420: 337-340

Takano J, Miwa K, Yuan L, von Wiren N, Fujiwara T (2005) Endocytosis and degradation of BOR1, a boron transporter of *Arabidopsis thaliana*, regulated by boron availability. Proc Natl Acad Sci USA 102: 12276-12281

Takano J, Wada M, Ludewig U, Schaaf G, von Wiren N, Fujiwara T (2006) The *Arabidopsis* major intrinsic protein NIP5;1 is essential for efficient boron uptake and plant development under boron limitation. Plant Cell 18: 1498-1509

Takano J, Tanaka M, Toyoda A, Miwa K, Kasai K, Fuji K, Onouchi H, Naito S, Fujiwara T (2010) Polar localization and degradation of *Arabidopsis* boron transporters through distinct trafficking pathways. Proc Natl Acad Sci USA 107: 5220-5225

Tanaka M, Sotta N, Yamazumi Y, Yamashita Y, Miwa K, Murota K, Chiba Y, Hirai MY, Akiyama T, Onouchi H, Naito S, Fujiwara T (2016) The minimum open reading frame, AUG-Stop, induces

boron-dependent ribosome stalling and mRNA degradation. Plant Cell 28: 2830-2849

Tanaka M, Takano J, Chiba Y, Lombardo F, Ogasawara Y, Onouchi H, Naito S, Fujiwara T (2011) Boron-dependent degradation of *NIP5;1* mRNA for acclimation to excess boron conditions in *Arabidopsis*. Plant Cell 23: 3547-3559

Uchiyama-Kadokura N, Murakami K, Takemoto M, Koyanagi N, Murota K, Naito S, Onouchi H (2014) Polyamine-responsive ribosomal arrest at the stop codon of an upstream open reading frame of the *AdoMetDC1* gene triggers nonsense-mediated mRNA decay in *Arabidopsis thaliana*. Plant Cell Physiol 55: 1556-1567

Uluisik I, Kaya A, Fomenko DE, Karakaya HC, Carlson BA, Gladyshev VN, Koc A (2011) Boron stress activates the general amino acid control mechanism and inhibits protein synthesis. PLoS One 6: e27772

von Arnim AG, Jia Q, Vaughn JN (2014) Regulation of plant translation by upstream open reading frames. Plant Sci 214: 1-12

Wakuta S, Mineta K, Amano T, Toyoda A, Fujiwara T, Naito S, Takano J (2015) Evolutionary divergence of plant borate exporters and critical amino acid residues for the polar localization and boron-dependent vacuolar sorting of AtBOR1. Plant Cell Physiol 56: 852-862

Wang S, Yoshinari A, Shimada T, Hara-Nishimura I, Mitani-Ueno N, Feng Ma J, Naito S, Takano J (2017) Polar Localization of the NIP5;1 Boric Acid Channel Is Maintained by Endocytosis and Facilitates Boron Transport in Arabidopsis Roots. Plant Cell 29: 824-842

Williamson LC, Ribrioux SP, Fitter AH, Leyser HM (2001) Phosphate availability regulates root system architecture in Arabidopsis. Plant Physiol 126: 875-882

Yamashita Y, Takamatsu S, Glasbrenner M, Becker T, Naito S, Beckmann R (2017) Sucrose sensing through nascent peptide-meditated ribosome stalling at the stop codon of *Arabidopsis bZIP11* uORF2. FEBS Lett 591: 1266-1277

Yoshinari A, Fujimoto M, Ueda T, Inada N, Naito S, Takano J (2016) DRP1-Dependent Endocytosis is Essential for Polar Localization and Boron-Induced Degradation of the Borate Transporter BOR1 in *Arabidopsis thaliana*. Plant Cell Physiol 57: 1985-2000

Yoshinari A, Takano J (2017) Insights into the Mechanisms Underlying Boron Homeostasis in Plants. Front Plant Sci 8: 1951

Zuckerkandl E, Pauling L (1965) Evolutionary divergence and convergence in proteins. Edited in Evolving Genes and Proteins by V. Bryson and H.J. Vogel, pp. 97-166. Academic Press, New York